Naval Research Laboratory
Washington, DC 20375-5000

NRL Memorandum Report 6244

Analysis of GEOSAT Radar Altimeter Errors Based on Pre-Launch Test Data

L. MILLER, A. ULIANA, J. SHUHY AND L. CHOY

Space Sensing Branch
Space Systems Technology Department

G. HAYNE AND D. HANCOCK

NASA Goddard Space Flight Center
Wallops Flight Facility
Wallops Island, VA 23337

June 28, 1988

SECURITY CLASSIFICATION OF THIS PAGE

REPORT DOCUMENTATION PAGE

Form Approved
OMB No. 0704-0188

1a. REPORT SECURITY CLASSIFICATION UNCLASSIFIED	1b. RESTRICTIVE MARKINGS
2a. SECURITY CLASSIFICATION AUTHORITY	3. DISTRIBUTION/AVAILABILITY OF REPORT Approved for public release; distribution unlimited.
2b. DECLASSIFICATION/DOWNGRADING SCHEDULE	
4. PERFORMING ORGANIZATION REPORT NUMBER(S) NRL Memorandum Report 6244	5. MONITORING ORGANIZATION REPORT NUMBER(S)
6a. NAME OF PERFORMING ORGANIZATION Naval Research Laboratory 6b. OFFICE SYMBOL (If applicable)	7a. NAME OF MONITORING ORGANIZATION
6c. ADDRESS (City, State, and ZIP Code) Washington, DC 20375-5000	7b. ADDRESS (City, State, and ZIP Code)
8a. NAME OF FUNDING/SPONSORING ORGANIZATION Space and Naval Warfare Systems Command 8b. OFFICE SYMBOL (If applicable)	9. PROCUREMENT INSTRUMENT IDENTIFICATION NUMBER
8c. ADDRESS (City, State, and ZIP Code) Washington, DC 20363-5100	10. SOURCE OF FUNDING NUMBERS PROGRAM ELEMENT NO. 63704N; PROJECT NO. X1596; TASK NO.; WORK UNIT ACCESSION NO.

11. TITLE (Include Security Classification)
Analysis of GEOSAT Radar Altimeter Errors Based on Pre-launch Test Data

12. PERSONAL AUTHOR(S)
Miller, L.S., Uliana, E.A., Choy, L.W., Shuhy, J., Hayne, G.S. and Hancock, D.W.

13a. TYPE OF REPORT	13b. TIME COVERED	14. DATE OF REPORT (Year, Month, Day)	15. PAGE COUNT
Final	FROM 8/86 TO 7/87	1988 June 28	61

16. SUPPLEMENTARY NOTATION

17. COSATI CODES			18. SUBJECT TERMS (Continue on reverse if necessary and identify by block number)
FIELD	GROUP	SUB-GROUP	GEOSAT Remote sensing; Radar altimeter; Automatic Gain Control (AGC)

19. ABSTRACT (Continue on reverse if necessary and identify by block number)

Prelaunch test results conducted on the GEOSAT radar altimeter ~~at Johns Hopkins University~~ Applied Physics Laboratory are discussed. This report is for documentation of results. The results are applicable to new sensor engineering design and testing, and post launch monitoring of performance degradation. These tests were to exercise the radar altimeter under: (1) conditions of transient and rapidly varying signal conditions, (2) nominal operating conditions, and (3) slowly varying conditions. The results have shown that the GEOSAT altimeter meets specifications, however, several subtle effects which will be important for designing future high precision altimeters are discussed. These effects relate to the temporal stability of the height, AGC, and waveform data; to interactions between AGC transients and height perturbations; and to height data statistics.

20. DISTRIBUTION/AVAILABILITY OF ABSTRACT	21. ABSTRACT SECURITY CLASSIFICATION
☒ UNCLASSIFIED/UNLIMITED ☐ SAME AS RPT ☐ DTIC USERS	UNCLASSIFIED
22a. NAME OF RESPONSIBLE INDIVIDUAL Lawrence W. Choy	22b. TELEPHONE (Include Area Code) (202) 767-2778 22c. OFFICE SYMBOL Code

DD Form 1473, JUN 86 *Previous editions are obsolete.* SECURITY CLASSIFICATION OF THIS PAGE

S/N 0102-LF-014-6603

CONTENTS

ANALYSIS OF GEOSAT RADAR ALTIMETER ERRORS BASED ON PRE-LAUNCH TEST DATA

1.0 INTRODUCTION

Prior to the launch of the GEOSAT satellite, prelaunch tests were conducted at Johns Hopkins University Applied Physics Laboratory (JHU/APL) on the radar altimeter to insure its proper operation and to determine various characteristics of the radar. At this same time, a special series of tests were conducted to examine the response of the altimeter to changes in AGC level, signal level, and simulated significant wave heights (SWH). These tests were conducted on 1 September, 8 September, 23 November 1983, and 4 December 1984, also referred to as test date I, test date II, test date III, and test date IV, respectively. All of the tests were made under ambient temperature conditions.

The purpose of these tests was to exercise the radar altimeter under: (1) conditions of transient and rapidly varying signal conditions such as those experienced by the radar altimeter under highly inhomogeneous ocean backscatter, (2) nominal operating conditions to acquire test data to be used to determine the degree of variance-reduction attainable as the data smoothing interval was increased, and (3) slowly varying conditions to study time-varying biases, and drift characteristics of waveform gate amplitude, height parameters, and derived quantities such as attitude angles and wind speed. The test plan is included in Appendix A.

The tests were conducted using the JHU/APL Radar Altimeter System Evaluator (RASE) to provide the input stimulus to the radar altimeter. The measured parameters, which were stored on magnetic tape, were later digitally processed and analyzed at the Naval Research Laboratory (NRL). The analysis treated the RASE and the radar altimeter as a single unit and any drift or change observed in the overall waveform characteristics could not be solely attributed to the altimeter, but might have been due to the RASE. Thus, the test results apply to the combined radar altimeter/simulator system.

This report is for documentation of results. The results are applicable to new sensor engineering design and testing, and post launch monitoring of performance degradation.

2.0 SUMMARY AND RECOMMENDATIONS

The GEOSAT radar altimeter functioned in a totally satisfactory manner relative to 10 cm altimetry and up to moderate (8 m) wave height simulations. The GEOSAT altimeter is an improved version of the SEASAT radar altimeter whose virtues are well known and have been successfully exploited in a number of different geodetic and oceanographic research projects [1,2]. The GEOSAT altimeter incorporated improvements in the data acquisition sequence and in the logic employed to track the radar return when the signal is losing lock.

Manuscript approved March 31, 1988.

The altimeter seems to have an altitude precision* of ~2 cm for 1-second averages of simulated 2 m SWH data, as compared to SEASAT whose corresponding precision was 3 cm under the same conditions.

The specific findings of these tests are as follows:

1. Overall, the test results showed considerable variation from one test date to another. During the first and last test dates, 9 September 1983 and 4 December 1984, the system at times displayed ~4 cm of altitude drift over an approximate 30 minute period. In addition, several waveform samplers (which sample each waveform in time increments of 3.125ηs) exhibited sizable variances [Table II] during the first test day. Also, covariance properties of the height data behaved anomalously; this would reduce the effectiveness of filtering techniques (e.g. Kalman filtering) which are used to process the operational altimeter data. These anomalous effects were essentially absent during the second and third test dates, 8 September 1983 and 11 November 1983. Although diagnostic tests were beyond the scope of this effort, there were indications that warm-up or tracker dynamics may have caused some of these effects. Such variations may represent inherent stability characteristics of the analog parts of the altimeter/simulator.

2. The tests conducted under dynamic AGC conditions indicated that variations in AGC may result in perturbations and time-varying means in the altitude data, especially for AGC levels <25db. This variation in the altitude data could effect the ability to measure small changes in surface topography since ocean current boundaries often exhibit changing σ^o behavior. A similar effect was noticed in SEASAT data, however, the "toggling" noted in SEASAT data [3] was not present in GEOSAT data and essentially has been removed by an improved GEOSAT system design.

3. An analysis of the random errors in the attitude data for test date I indicated that a 10 second averaging interval of the waveform used to determine V_{att} was needed to attain an altitude uncertainty of $\leq$2 cm, and a 60 second averaging interval of V_{att} was needed to attain a 0.1dB resolution in σ^o. While the 10 second averaging period of the waveform used to determine V_{att} is of little consequence, since the satellite would only travel about 70 km in 10 seconds, the 60 second interval is considered excessive due to the potentially large spatial variability with respect to wind speed. The corresponding averaging periods needed to achieve the above mentioned resolutions from test date III were far shorter, 6 seconds and 30 seconds respectively.

4. In general, the altitude and waveform data contained fluctuations considerably in excess of the expected levels based on Rayleigh waveform statistics. In effect, variance of the altimeter data products did not change inversely with averaging period, as the Rayleigh theory indicates it should. This suggests that extraneous low-frequency noise, or drift, was present in these data. These fluctuations were evident in the data from test date I for both the mean waveforms and the tracker covariances.

*Precision is taken to be the 1σ uncertainty arising from the short-term random fluctuations in the height data. Intermediate to long-term repeatability is not implied.

5. During the test date IV both the primary and back-up microprocessors on GEOSAT were used during the special tests. No discernable differences were observed in the resulting data analysis. This is important in the event that back-up processors ever have to be used as a result of failure of the primary processor during flight.

3.0 ALTITUDE DATA CHARACTERISTICS

The covariance of the 10/sec height data for test date I is shown in Figure 1. The covariance decreased to a value of ~.55 for unity lag and then varied about zero in a non-descript manner for other lags. This behavior was expected since the 10/sec height data from the altitude tracker represented a low-pass process with a cutoff of ~5 Hz. The autocovariance values for both the 10/sec and 5 second averaged altitude data for test date I and the 5 second averaged altitude data for test date IV are shown in Figures 2A and 2B respectively. Note the substantial degree of correlation present in the 5 second averaged altitude data on test date IV. (Subsequent processing of the test date III averaged altitude data showed these data to be uncorrelated as shown in Table 1.)

The standard deviation of the altitude data was examined as a function of the averaging period. The results (Figure 3) for the standard deviation calculation, which assumed a non-time-varying mean value, showed higher standard deviation values than expected for the time averaged data. First order regression calculations were then conducted to test for the presence of a linear rate with negative results. Higher order regression calculations were subsequently made which indicated a mean-value trend in the data. A 4th degree polynomial regression reduced the altitude standard deviation by ~16 percent (as shown in Figure 3). This variance reduction was attributed to slowly varying changes in mean value during the test, such as that shown in Figure 4A and 4B. Test date III data did not exhibit this characteristic (see Figure 4C).

The 10/sec and 5 second averaged altitude time series data for test date IV is shown in Figures 5A and 5B starting at a time of 17:36:36 when the height rate was set at 25 m/sec. Periodic variations were noted in the 10/sec data and an autocovariance function for these data showed a cyclic correlation for a lag of ~80 values (Figure 5C), which corresponds to an ~0.13 Hz low frequency component.

Two anomalies noted in the altitude data correlation properties were: (1) the sustained correlation values for all lags in the 5 second filtered time series during periods of drift in the altitude data (Figure 2B); and (2) periodicities in the correlation properties of the 10/sec altitude data which resemble an underdamped tracker condition (Figure 5C). This effect was more pronounced when the 25 m/s altitude rate was present.

A power spectrum for the height data during the test date IV data is shown in Figure 6. Note the presence of an apparent exponential decay from 0-5 Hz, and several power spikes, the largest of which appear to correspond to 0.13 Hz, the same frequency to which periodicities in the autocovariance function of the 10/sec altitude data corresponded in Figure 5C. The exponential decay seen in the power spectra is somewhat surprising since the overall spectral shape should be determined by the Rayleigh fading nature of

TABLE I

Autocovariance function of 5 second-average altitude data

	Test Date III Test 1A and 2B	Test Date I Test 1A and 2B
LAG	ACF	ACF
0	1.0	1.0
1	.164	.570
2	-.016	.536
3	.051	.574
4	.102	.512
5	-.004	.538
6	-.049	.543
7	.059	.499
8	.068	.501
9	.015	.497
10	-.002	.492
11	.010	.496
12	.066	.492
13	.082	.472
14	.101	.491
15	.049	.471
16	.059	.446
17	-.011	.480
18	-.031	.414
19	.025	.448
20	.026	.439

the waveforms and would be expected to approximate white-noise in the low frequency limit. The cause for this departure is probably attributable to characteristics of the RASE simulator.

The AGC level for test date I and test date III exhibited a continual downward drift throughout the tests (Figure 7 and 8). The AGC values were subsequently temperature corrected using the results of the thermal-vacuum tests described in Appendix B. After applying the temperature correction, the trend was removed and the standard deviation of the mean value of the one second averages of AGC was then only 0.05 dB.

Several tests were conducted in which the signal level attenuator of RASE was changed and the response of AGC was monitored. During these tests the attenuation was either changed manually, or through a programmed time varying sequence to test for AGC linearity and any altitude perturbations that might be present. These tests were conducted to verify the improvements which had been made to improve GEOSAT AGC performance over that of SEASAT. The results were quite positive and are detailed in Appendix C. The pronounced irregular "steppiness" and unstable "toggling" regions seen in the SEASAT radar altimeter were absent from GEOSAT. The data showed good linear response over much of the AGC range with a smooth reasonable departure from linearity only at low AGC levels and suggested that the AGC measurement error was not appreciably worse than 0.1 dB.

The tests for possible interaction between AGC transients and altitude disturbances were far less conclusive. Typical altitude and AGC time histories are shown in Figures 9-12. The altitude record for test date III showed glitches labeled A, B, and C in Figure 9A which appear to be associated with large changes of AGC (about 30 dB) over a short time period (~10 sec) and with AGC values of less than 15 dB as seen in Figure 9B. The third event, labeled C, was in the opposite direction of altitude from events A and B. A similar result is seen in data from the test date IV data (Figure 10). The perturbation in altitude appears to be associated with a 20 dB change in AGC in less than 10 sec. Two smaller changes in AGC of about 10 dB did not seem to have much effect on the altitude value. Two other time histories are shown in Figures 11 and 12 for times when the AGC was manually changed. In both of these cases the change in AGC was gradual over time and little response was noted in the altimeter value. The magnitude of altimetric effects discussed above are well within GEOSAT performance specifications, the largest being about 6 cm as was seen in the test date III and test date IV data (Figures 9A and 10). These types of effects were observed in SEASAT during its operational mission. Quoting from Townsend [1]:

> "Another type of anomaly has been demonstrated... to be due to passage over an intense raincell in open ocean. In this case, the effect is evidence by a decrease in AGC due to signal attenuation through the raincell, followed by a change in height, and an increase in SWH."

Similar waveheight effects were noticed in this analysis. Time histories for AGC and SWH are shown in Figures 13A and 13B. The test results indicated a correlation between large AGC transients (~25 dB) over a short

time period (~10 sec), and SWH perturbations. Further testing in this area is needed to quantify the effect of AGC transients on altitude and SWH.

4.0 WAVEFORM RELATED TEST RESULTS

A 36 second average was calculated on the waveform data for the test date I test data (Figure 14A). A special set of gain calibration constants was used for the sampling gates to essentially remove the so called droop at the end of the average waveform which had been noted in the SEASAT altimeter data [1,4,5]. However, when the waveform calibration data were used to correct the data from the test date III data, the late-waveform decay was still present (Figure 14B).

There were other waveform sample anomalies noted in the test date I data. As seen in Table II, sample number -16, and to a lesser extent sample numbers -8 and -24 had dc offsets and high values of standard deviation. The average value for sample number -16 was approximately twice that of the neighboring values and the standard deviation about five times larger than the baseline values. Since the Rayleigh thermal, or time-sidelobe noise in the simulated waveforms could hardly vary on an individual sampler basis, the high standard deviation suggests a slowly varying gain instability in sample number -16 data.

Two waveforms which were obtained approximately seventy minutes apart during the test date IV tests are shown in Figures 15A and 15B. The waveform in Figure 15A corresponds to a simulated 2 m wave height, a 25 m/s height rate, and a low signal-to-noise ratio. An AGC step change of 10 dB was then added to the system resulting in the waveform shown in Figure 15B. A comparison of the two waveforms shows a difference in the late-gate values. This difference in the late-gates corresponded to an attitude angle difference of approximately 0.3 degrees. It should be pointed out that a 10 dB change in AGC is probably larger than would be expected during normal operation of the altimeter.

Uncertainty in the attitude angle is critical because of its effect on the height determination, σ^o, and wind speed values. The relationships for this uncertainty are [5,6]:

$$\Delta h = 234(\Delta V_{att}) \quad \text{cm/volt} \tag{1}$$

and

$$\Delta AGC = 30.12(\Delta V_{att}) \quad \text{dB/volt} \tag{2}$$

where Δh, ΔV_{att}, and ΔAGC are the height, attitude voltage, and AGC increments respectively. Equation (1) corresponds to a significant wave height of 16 m. For a SWH of 8 meters, $\Delta h = 108(\Delta V_{att})$ which shows the influence of SWH on Δh. Both (1) and (2) are for an attitude angle near 0 degrees. Aside from the effects of the receiver thermal noise, the stabilities of the V_{att} estimates in expressions (1) and (2) are a function of the waveform statistics, not of the significant wave height. This insensitivity of V_{att} to wave height changes can be understood by referring to Figure 16. This figure shows the attitude (or late) gate values to be essentially independent of sea state.

Table II

SAMPLE	MEAN	STD DEV	SAMPLE	MEAN	STD DEV
-30	7.94	1.54	1	112.75	12.67
-29	5.34	1.98	1.5	130.77	13.03
-28	7.86	1.29	2	145.66	14.23
-27	5.42	1.15	3	162.72	16.68
-26	5.67	1.13	4	177.11	17.01
-25	6.76	1.21	5	178.64	15.90
-24	7.78	4.40	6	182.2?	16.81
-23	6.45	1.22	7	186.??	5.35
-22	6.51	1.21	8	185.??	1?.70
-21	6.51	1.87	9	182.?3	17.83
-20	6.89	1.47	10	185.??	?7.55
-19	7.08	1.29	11	178.69	.4.78
-18	6.95	1.12	12	175.97	19.66
-17	6.95	1.84	13	176.16	17.87
-16	12.37	6.91	14	175.09	13.95
-15	6.26	1.33	15	172.91	15.11
-14	7.32	1.31	16	172.49	15.71
-13	6.68	1.19	17	170.83	17.50
-12	6.24	1.38	18	164.87	18.76
-11	7.49	1.38	19	167.31	16.00
-10	7.32	1.23	20	162.62	14.62
- 9	6.69	1.78	21	159.69	14.23
- 8	9.99	4.02	22	163.96	16.55
- 7	9.33	1.66	23	158.94	17.23
- 6	9.65	1.55	24	158.32	16.76
- 5	16.32	1.40	25	157.67	14.73
- 4	14.99	1.81	26	153.37	13.58
- 3	13.95	2.11	27	154.25	11.25
- 2	32.14	3.52	28	157.44	17.31
- 1.5	39.66	4.47	29	151.21	17.02
- 1	64.49	6.59	30	155.64	15.30
- 0.0	82.88	9.16			

A close examination of the waveforms shown in Figures 17-20 indicated that the overall slope of the plateau was slightly dependent on the signal level (AGC). Waveforms for a simulated wave height of 8 meters is represented in Figures 17 and 18 (test date II) and waveforms for 2 meter simulated wave height in Figures 19 and 20 (test date III). The AGC values for the waveform shown in Figures 19 and 20 were 25 dB and 44 dB respectively yielding V_{att} values of 1.769 and 1.794. This resulted in a change in the attitude angle of approximately 0.25° near nadir which would yield significant errors in the wind speed calculation. An examination of all the available waveforms showed the greatest plateau slope sensitivity to occur at AGC levels <25 dB.

The test data were also examined for possible excess noise in V_{att} and its effect on height, h, and AGC. In order to assess this noise in V_{att} as a function of the averaging interval, the test date I data were processed to yield waveforms averaged over 5, 30, and 210 seconds. These waveforms were then used to determine V_{att}. The results are shown in Appendix D. The standard deviation of the V_{att} values were 0.0125, 0.005, and 0.0035 for the 5, 30, and 210 second averaging periods respectively. Values of Δh and ΔAGC based on equations (1) and (2) are given in Table III.

TABLE III

Averaging Period (Sec.)	ΔV_{att} Measured	Δh (cm)	ΔAGC (dB)	ΔV_{att} Computed
5	.0125	2.92	.377	.01
30	.005	1.17	.15	.004
210	.0035	.819	.105	.002

Interpolating between values, an averaging period of V_{att} of approximately 10 sec would be required to reduce the Δh error to 2 cm and an averaging period of approximately 60 seconds would reduce the ΔAGC to 0.1 dB. These interpolated values of 10 and 60 seconds were obtained by scaling the 5 sec values by the square root of the ratio of the averaging periods.

Estimates of the standard deviation of the attitude gate based on the Rayleigh model (assuming 6 uncorrelated samples and scaling to a mean value of $V_{att} \simeq 1.8$) are also shown in Table III. Note that this method does not take into account uncertainty in the AGC gate which is formed from all 60 waveform samples. This procedure yielded an excess-over-Rayleigh noise factor of 1.25 and 1.75 for the 5 and 210 second averages respectively for the test date I results; values for the test date III data were very close to the Rayleigh estimate.

These test results have shown that the GEOSAT altimeter meets specifications, but have uncovered several subtle effects which will be important in the future when designing higher precision altimeters. These effects generally relate to the temporal stability of the height, AGC, and waveform data; to interactions between AGC transients and height perturbations; and to height data statistics.

Due to a launch schedule which precluded follow-up testing, these results are considered to be indicative rather than definitive. It is possible that effects such as height drift can be correlated with sub-system temperatures. Also, these test results apply to the combined RASE/altimeter system.

5.0 ACKNOWLEDGEMENTS

We wish to acknowledge the friendly and able cooperation given to us by John McArthur and Paul Martin of the Johns Hopkins Applied Physics Laboratory throughout these pre-launch tests. The support and encouragement given by Dr. Vincent Noble of NRL is greatly appreciated. This work was funded by the Space and Naval Warfare Systems Command. We wish to thank Ms. Linda Ridgely and Mrs. Kathleen Funk for the typing of the entire manuscript.

6.0 REFERENCES

1. W. Townsend, "An initial assessment of the performance achieved by the SEASAT 1 radar altimeter", IEEE Jour. of Ocean Eng., Vol. OE5, April 1980.

2. "SEASAT Special Issue II: Scientific Results", JGR, Vol. 88, No. C3, February 1983.

3. D. B. Chelton and McCabe, P. J., "A review of satellite altimeter measurement of sea surface wind speed: With a proposed new algorithm", JGR, 90, 1985.

4. G. S. Hayne, "Wallops waveform analysis of SEASAT 1 radar altimeter data", NASA CR 156869, July 1980.

5. L. Miller, "A review of the GEOSAT radar altimeter system", interim report on Contract No. N00014-82-M-0187, Applied Science Assoc., December 1982.

6. J. McArthur, APL private communication.

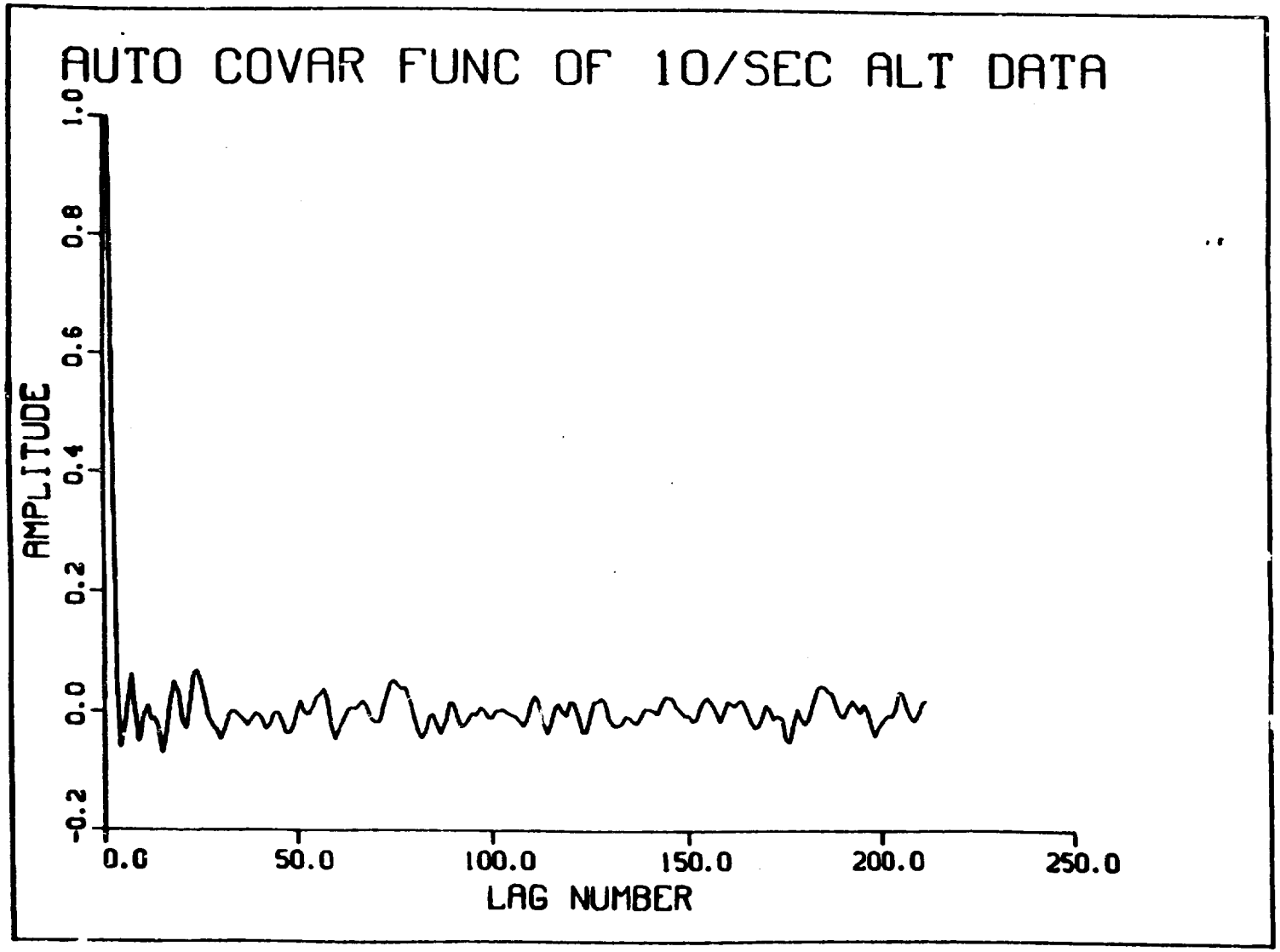

Fig. 1 — Auto-covariance of 10/sec. height data, 9-1-83 test

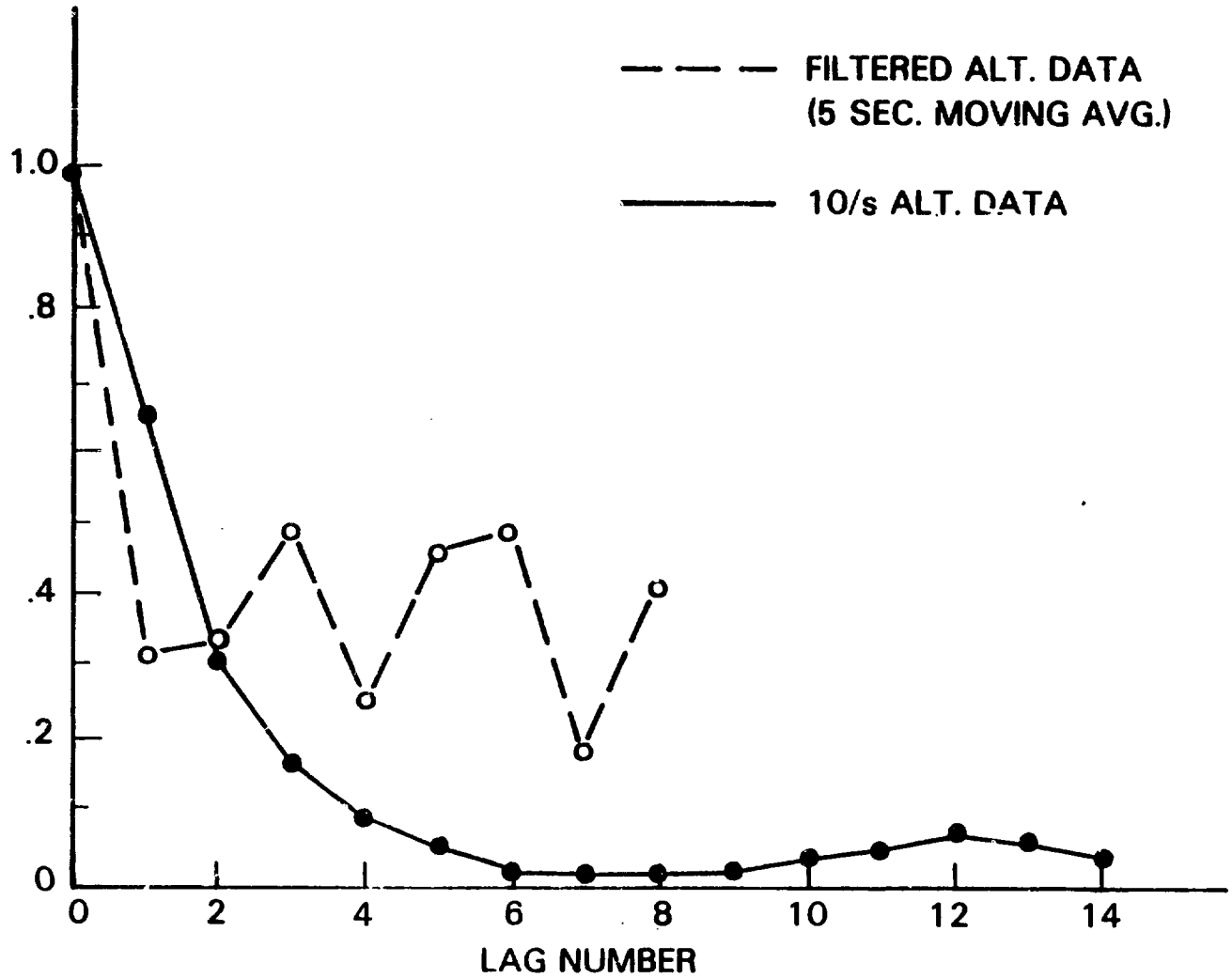

Fig. 2a — Covariance functions of altitude data for 9-1-83 test

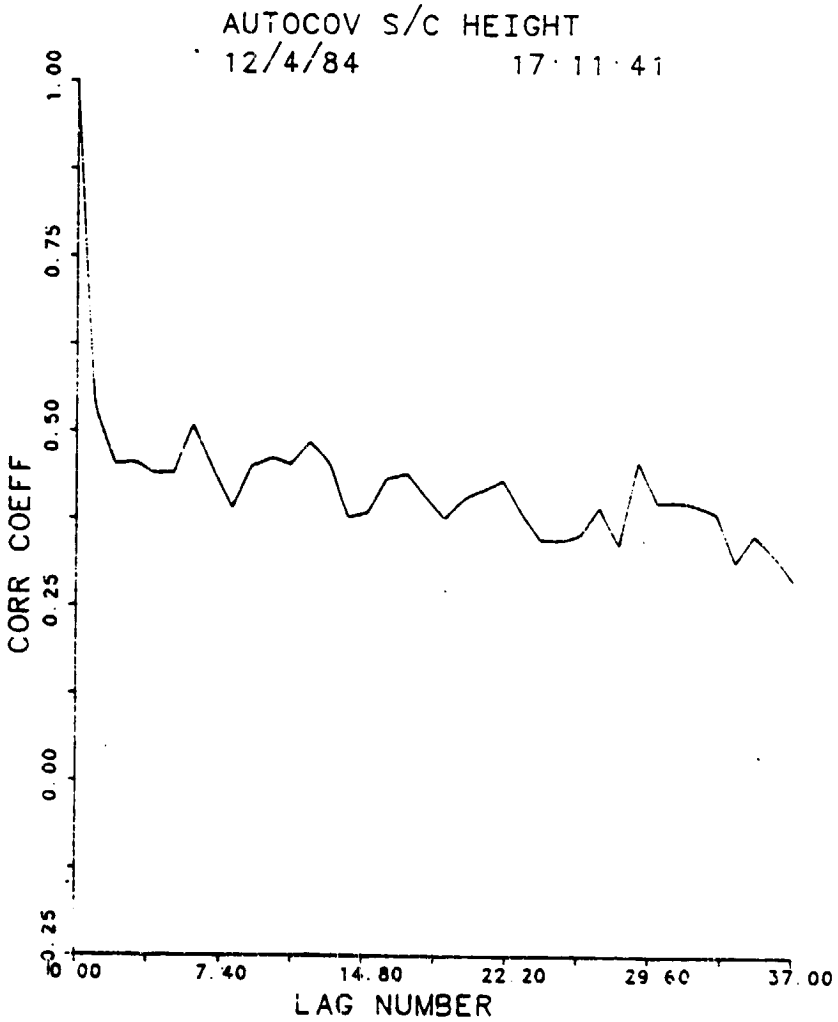

Fig. 2b — Covariance function of altitude data for 12-4-84 test

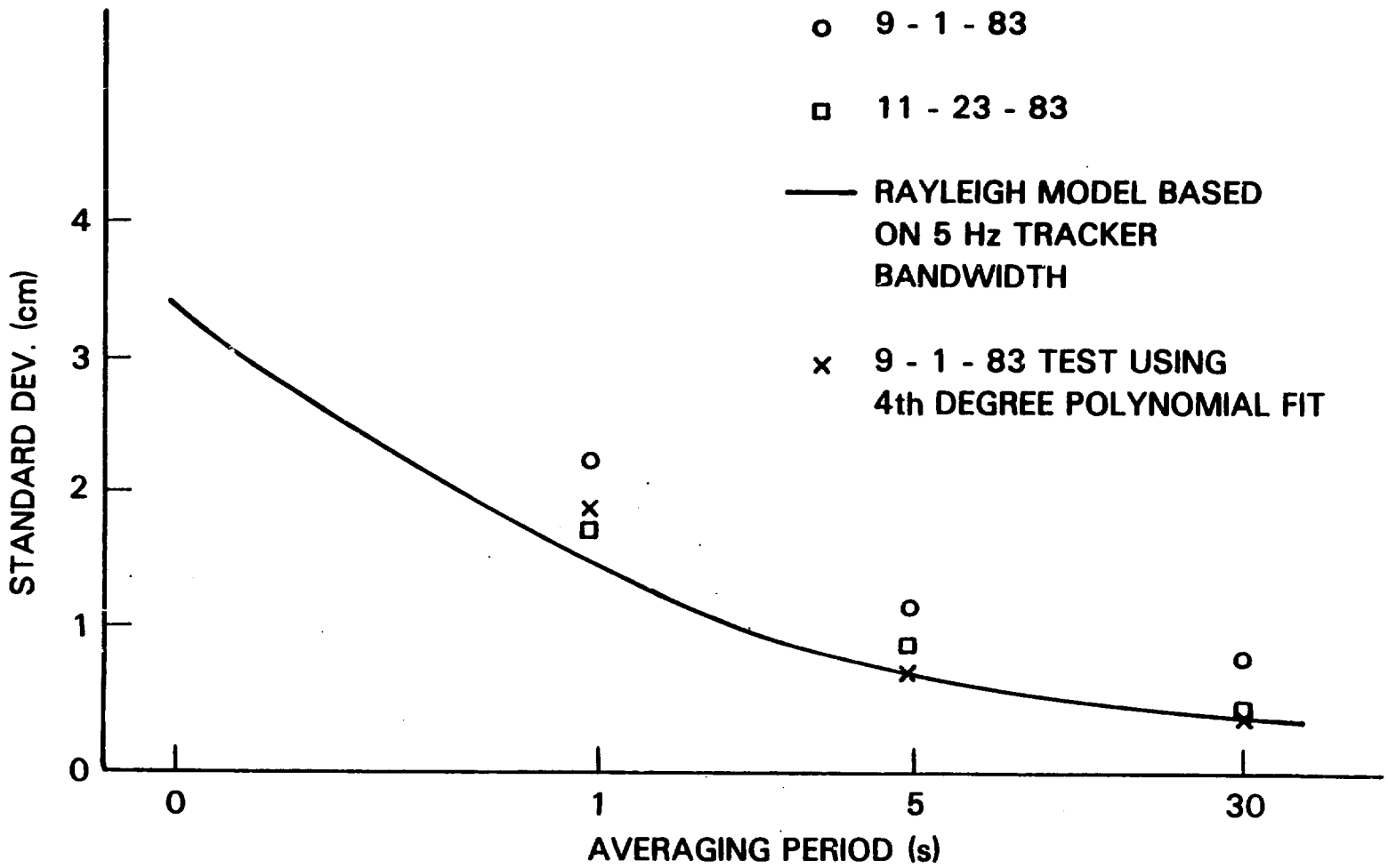

Fig. 3 — Height data standard deviation vs averaging period, for constant AGC level

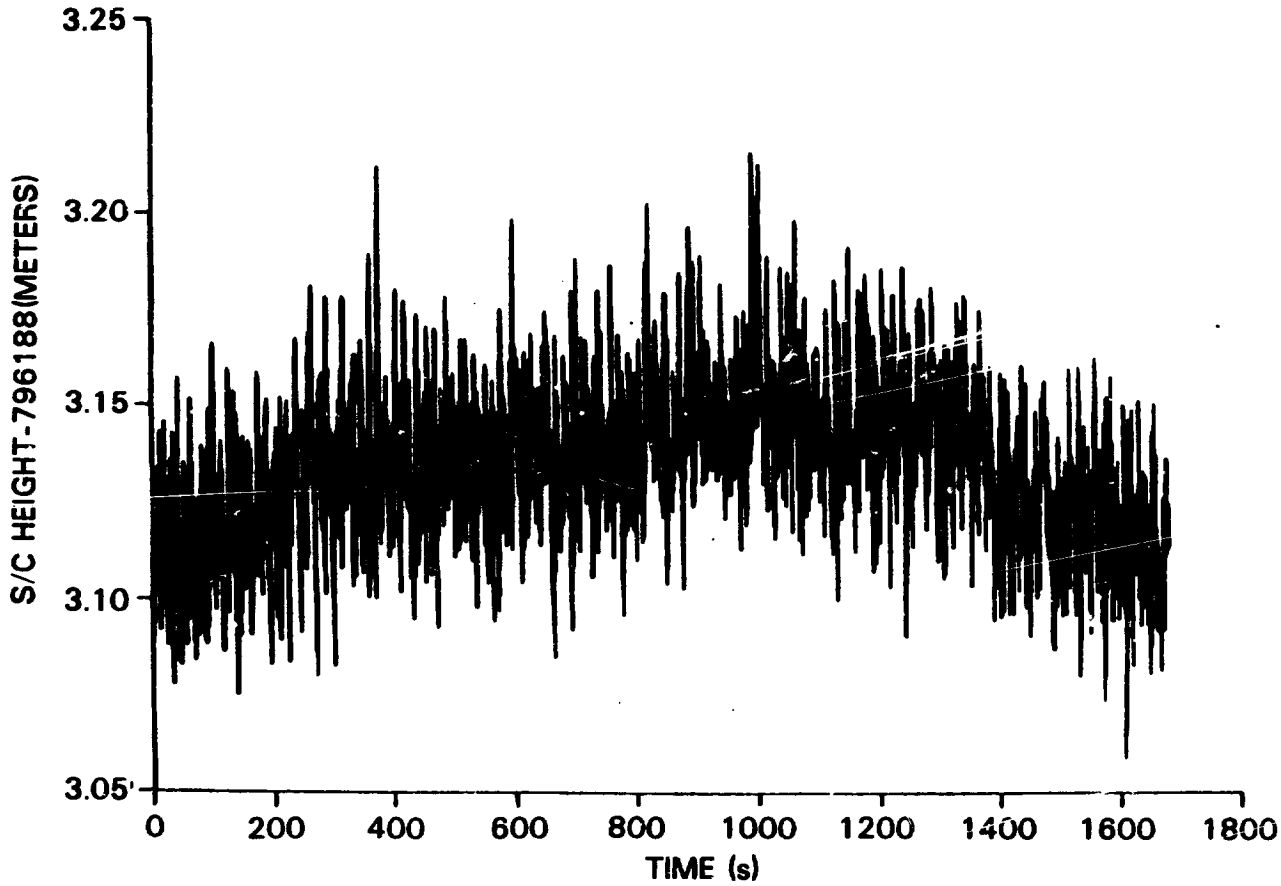

Fig. 4a — One-second averaged height data, 9-1-83 test

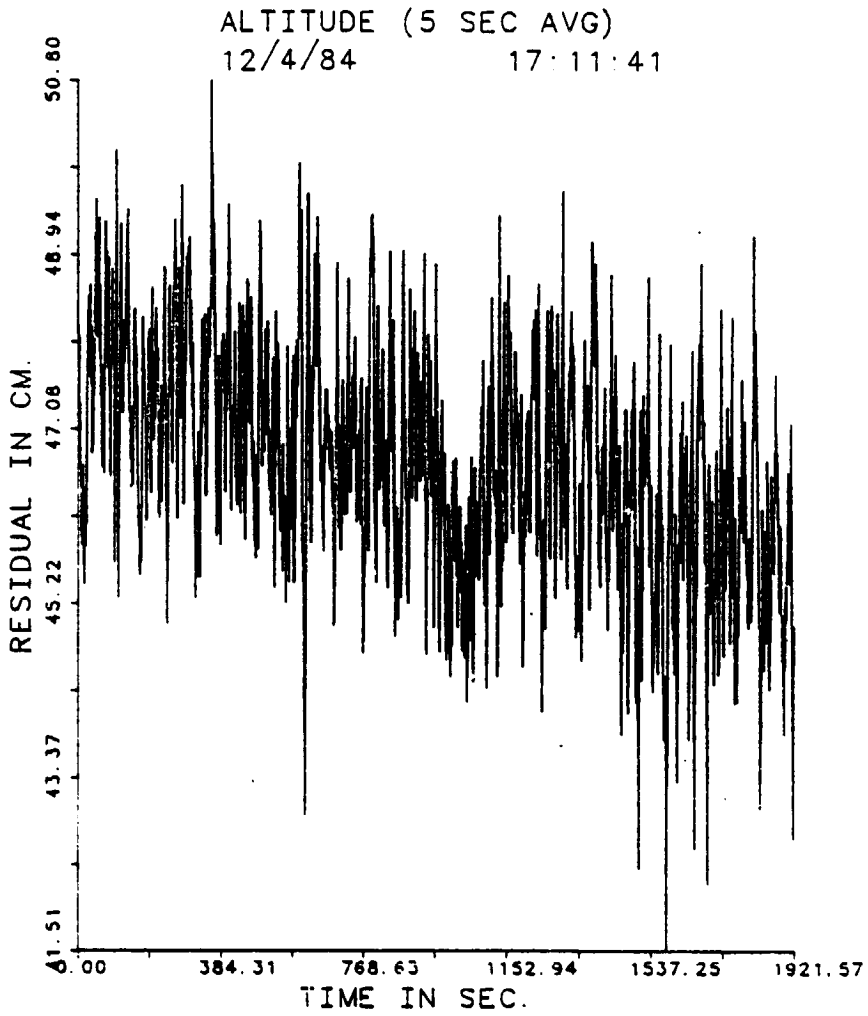

Fig. 4b — Five-second averaged height data — 12-4-84 test

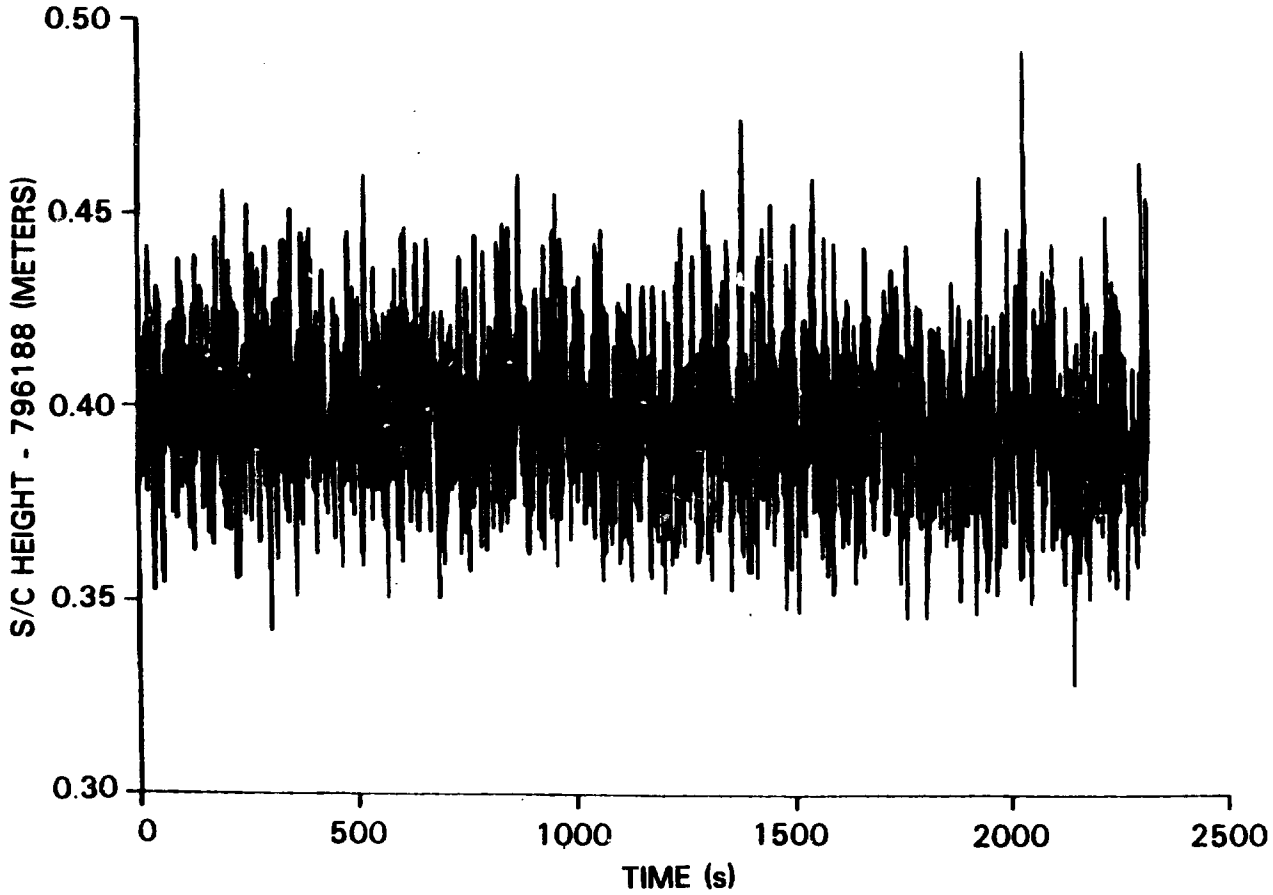

Fig. 4c — One-second averaged height data, 11-23-83 test

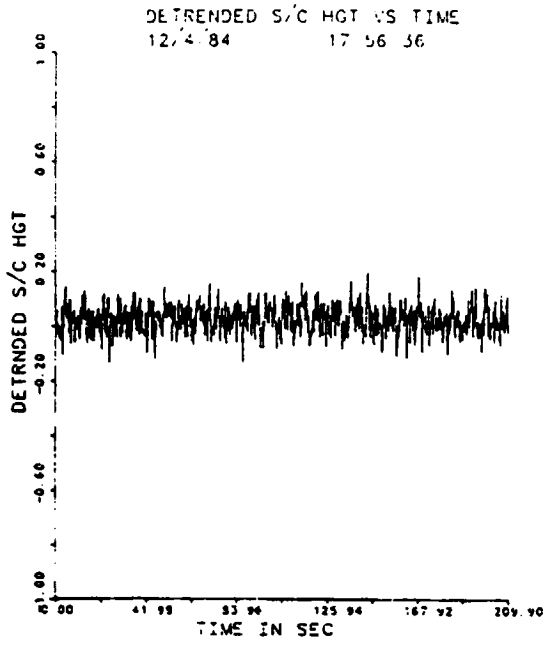

(a)

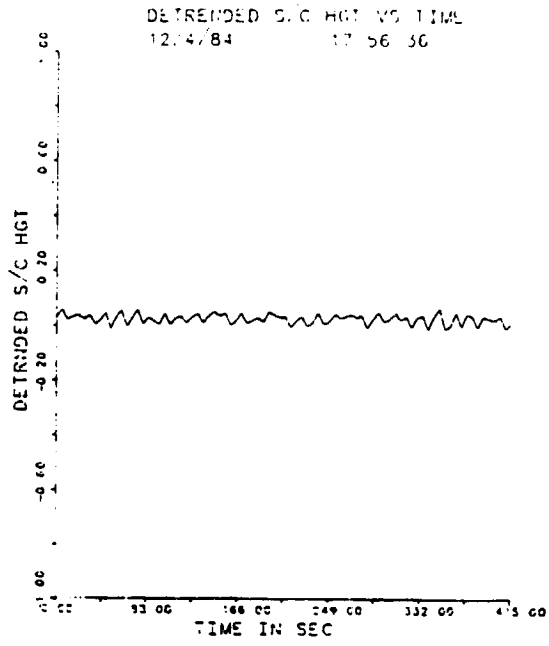

(b)

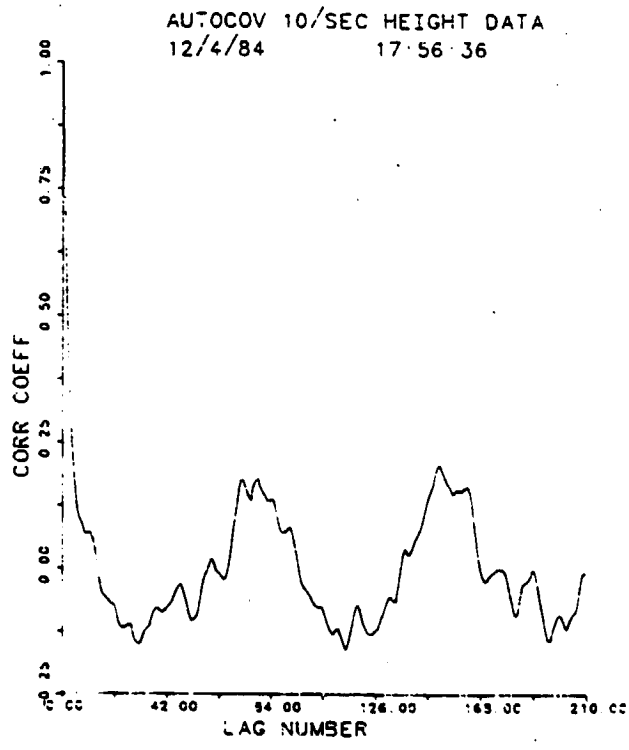

(c)

Fig. 5 — Altitude data characteristics during period in which low-frequency variations were present.

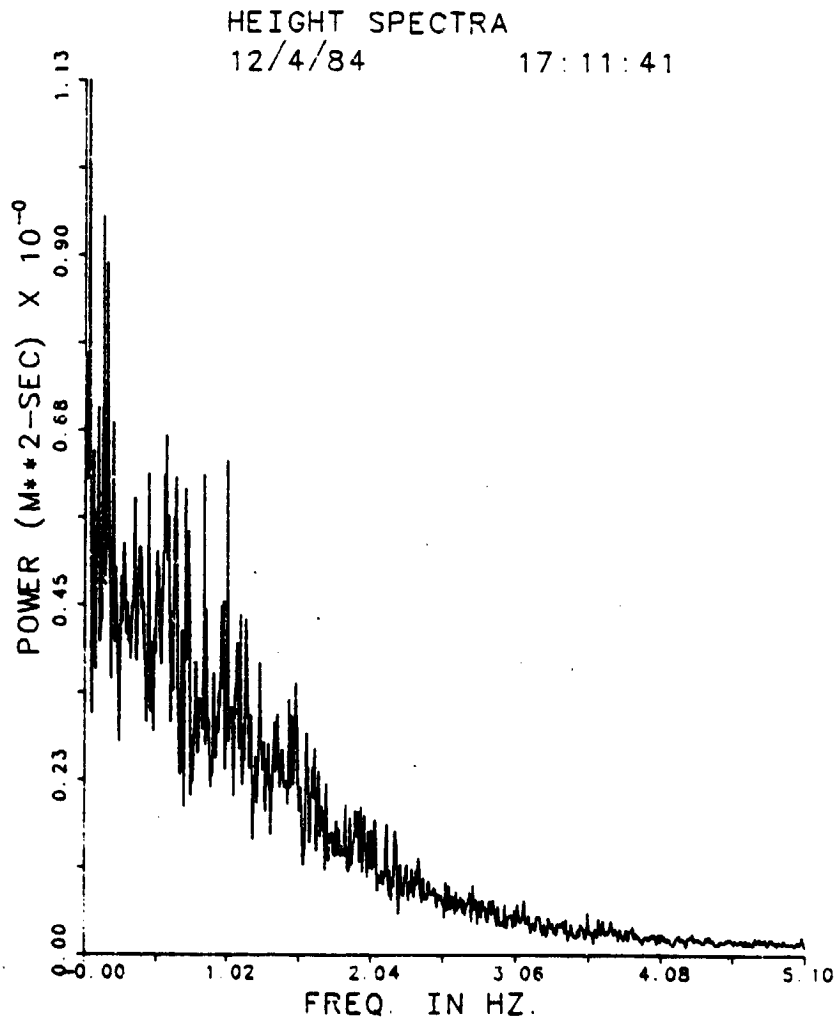

Fig. 6 — Power spectral density of 10/s. altitude data, 12-4-84 test

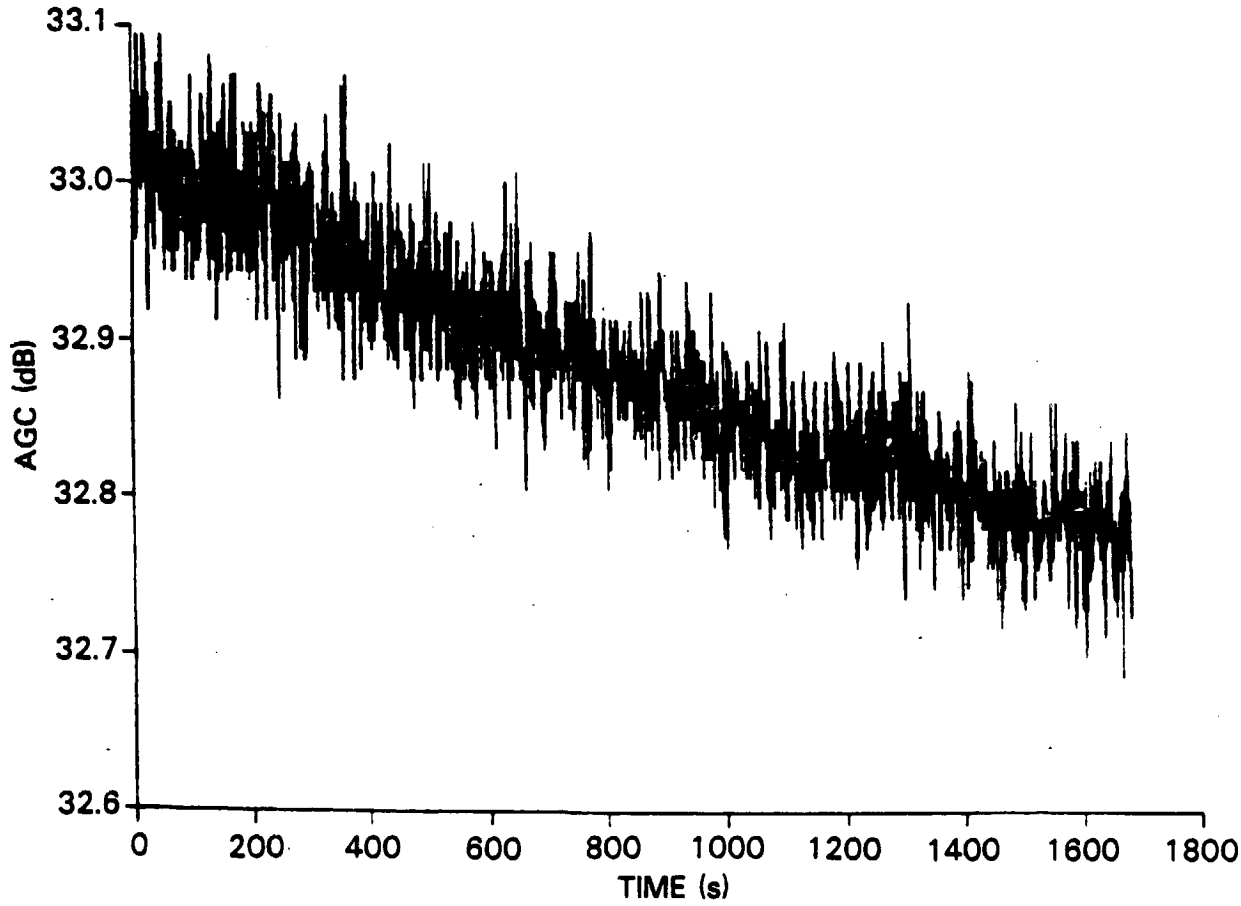

Fig. 7 — AGC record for 9-1-83 test

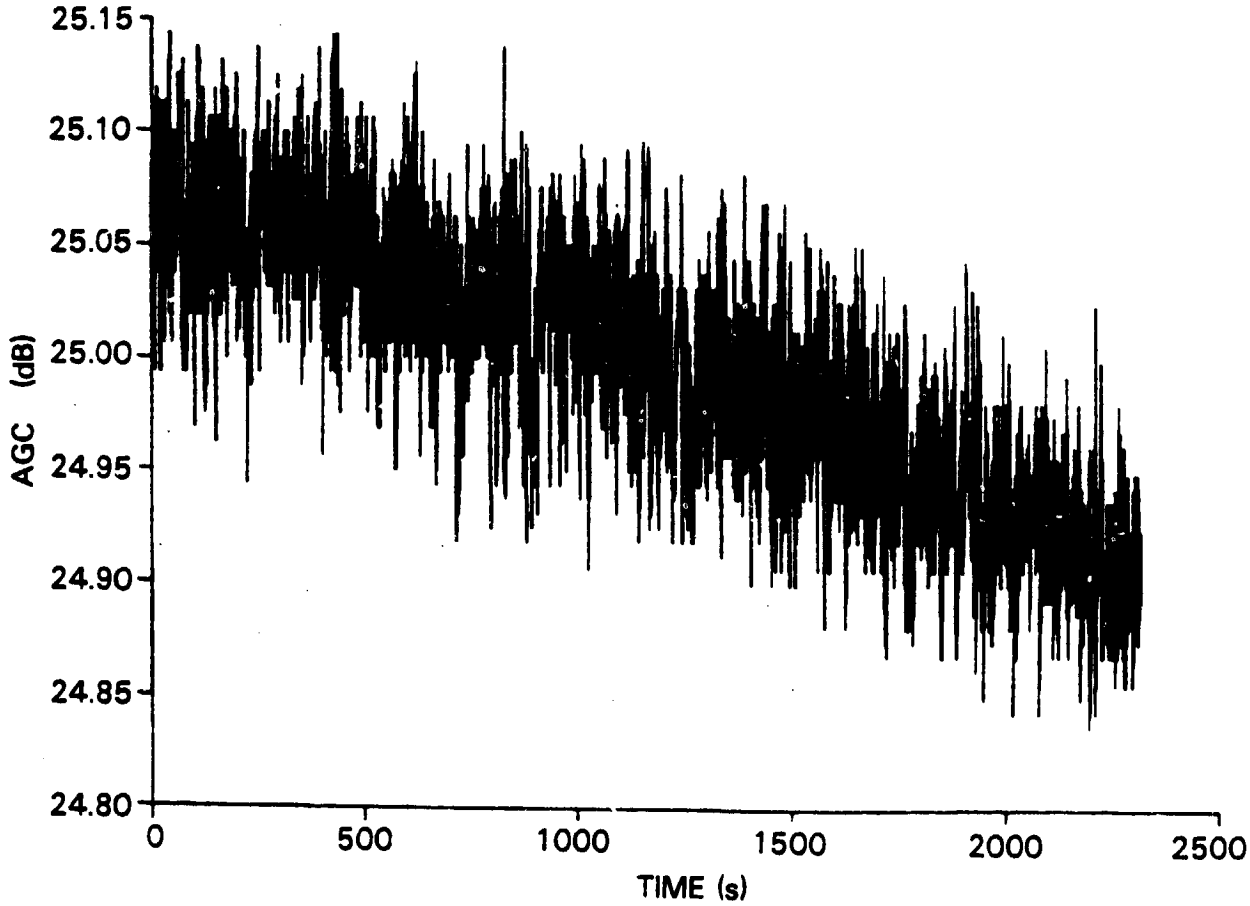

Fig. 8 — AGC record for 11-23-83

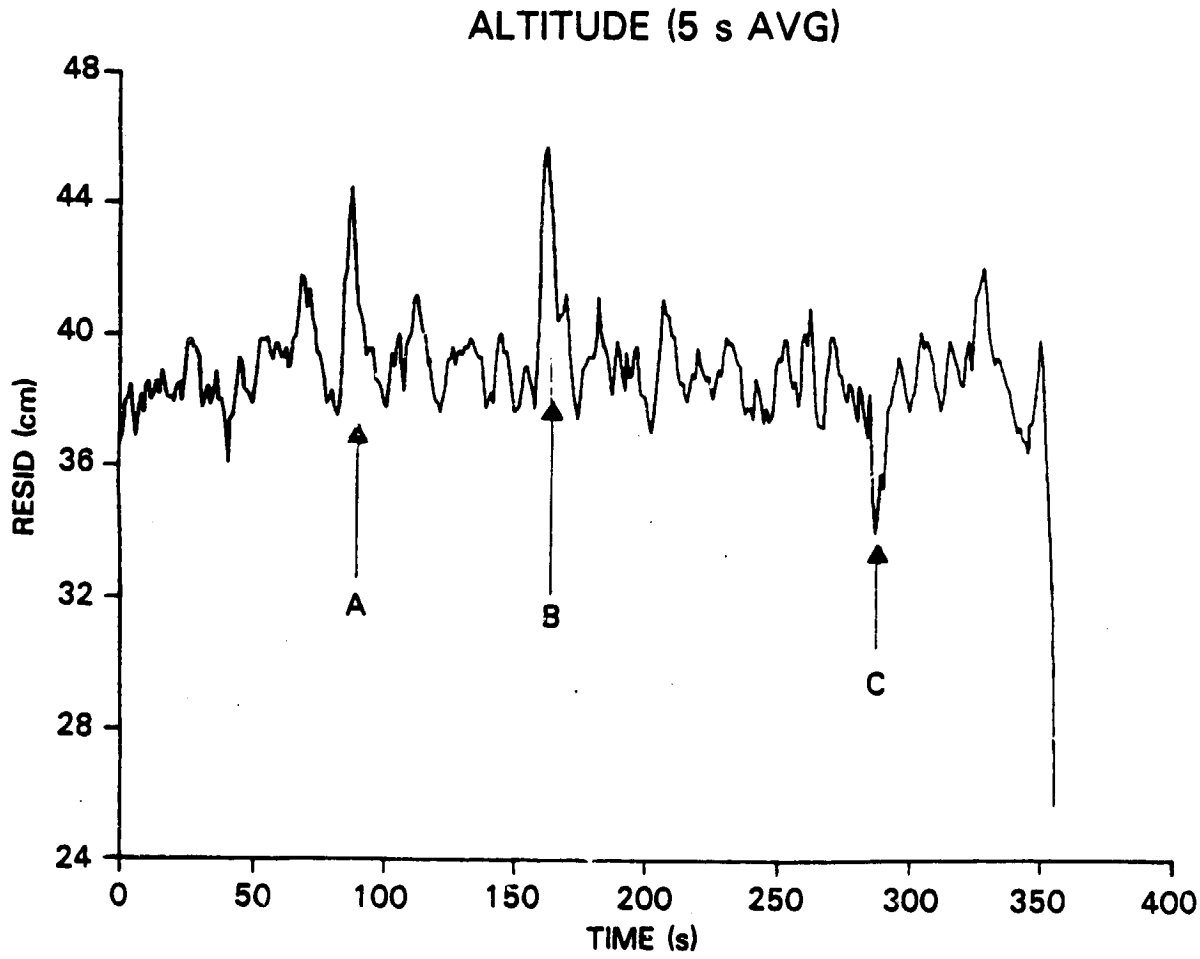

Fig. 9a — Altitude disturbances (A,B,C) correlated with AGC transients (A,B,C) for 11-23-83 data

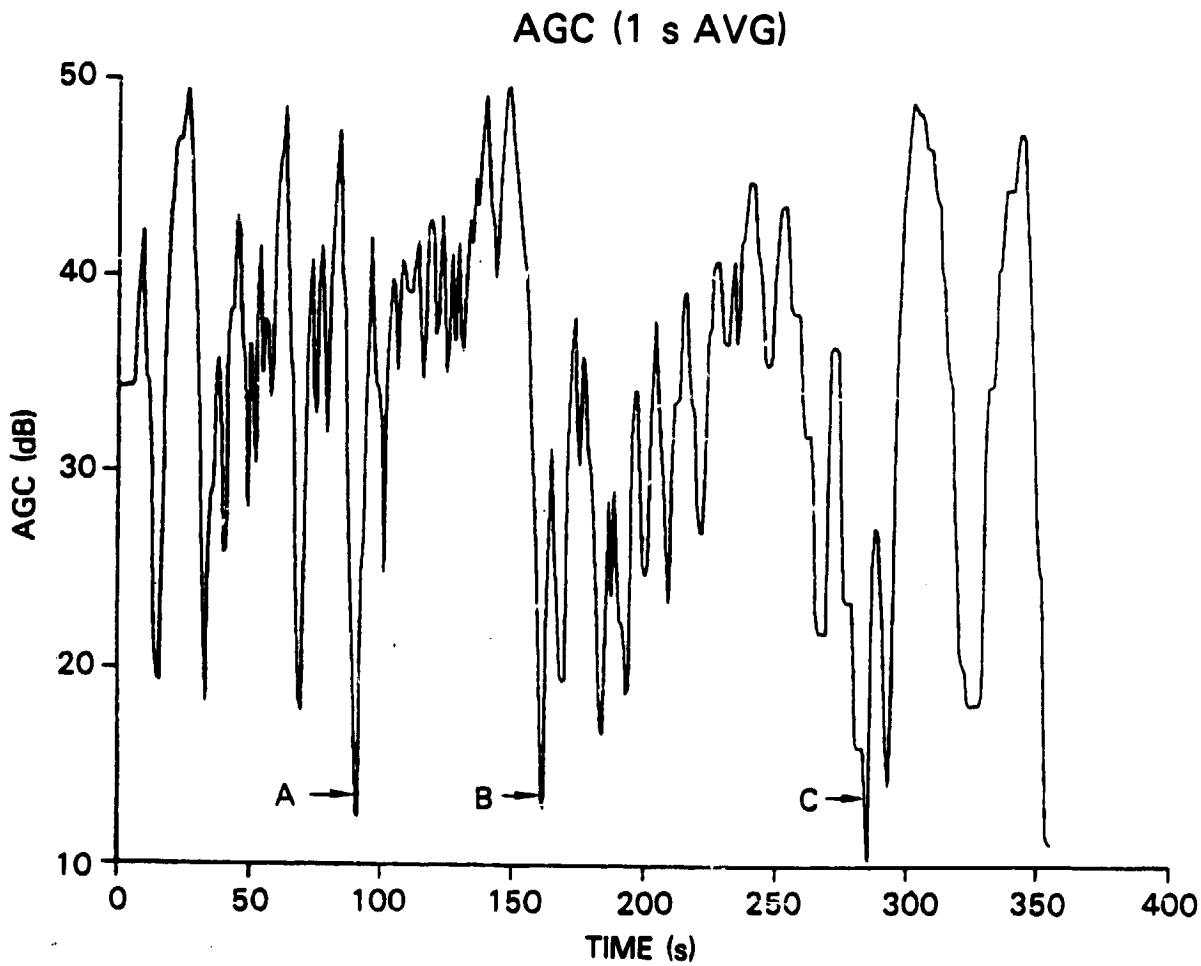

Fig. 9b — Altitude disturbances (A,B,C) correlated with AGC transients (A,B,C) for 11-23-83 data

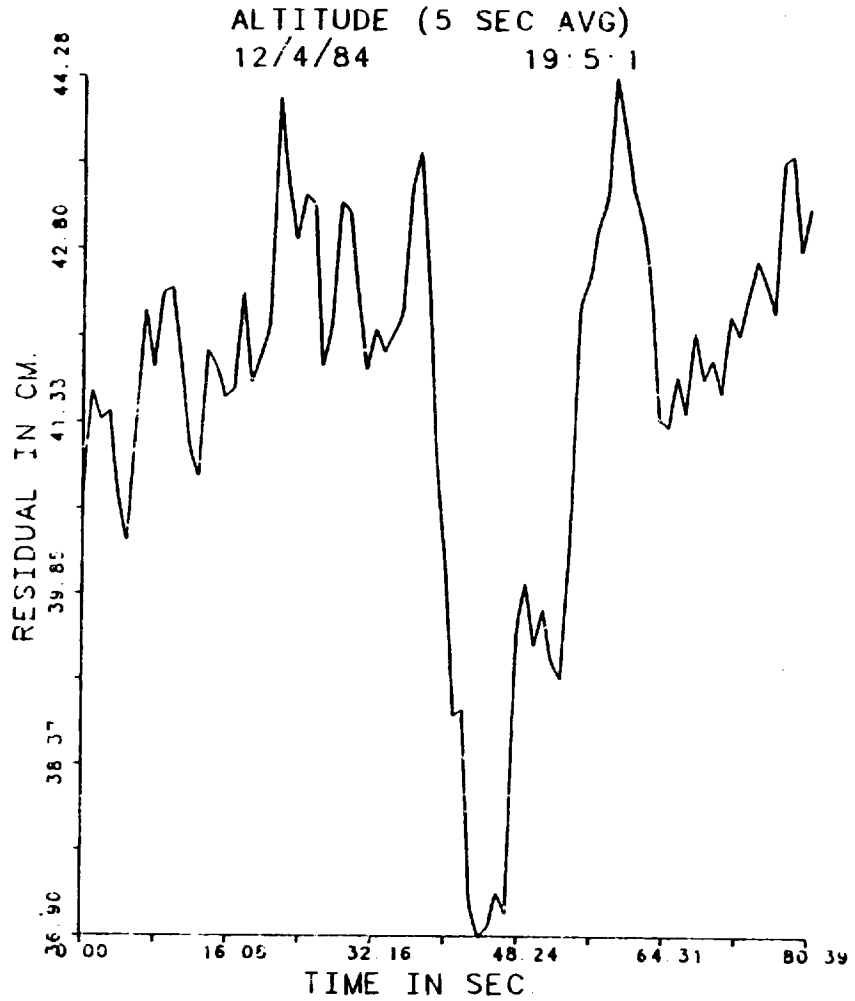

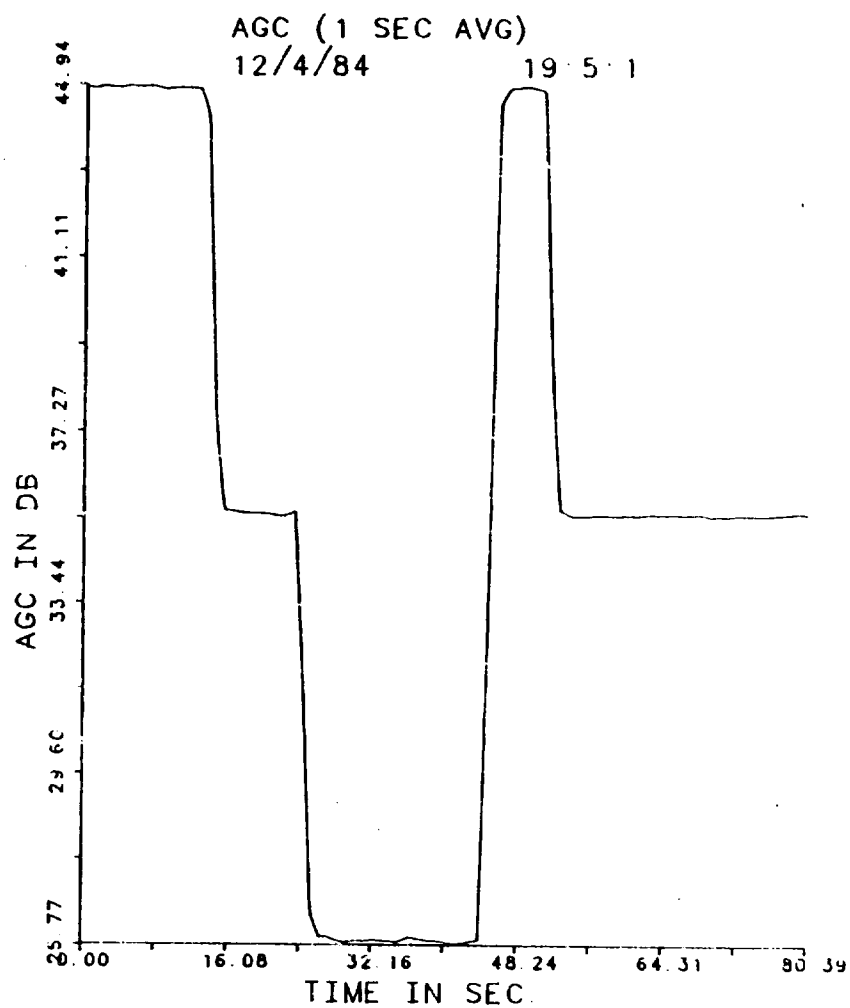

Fig. 10 — Altitude disturbance correlated with AGC variations for 12-4-84 data

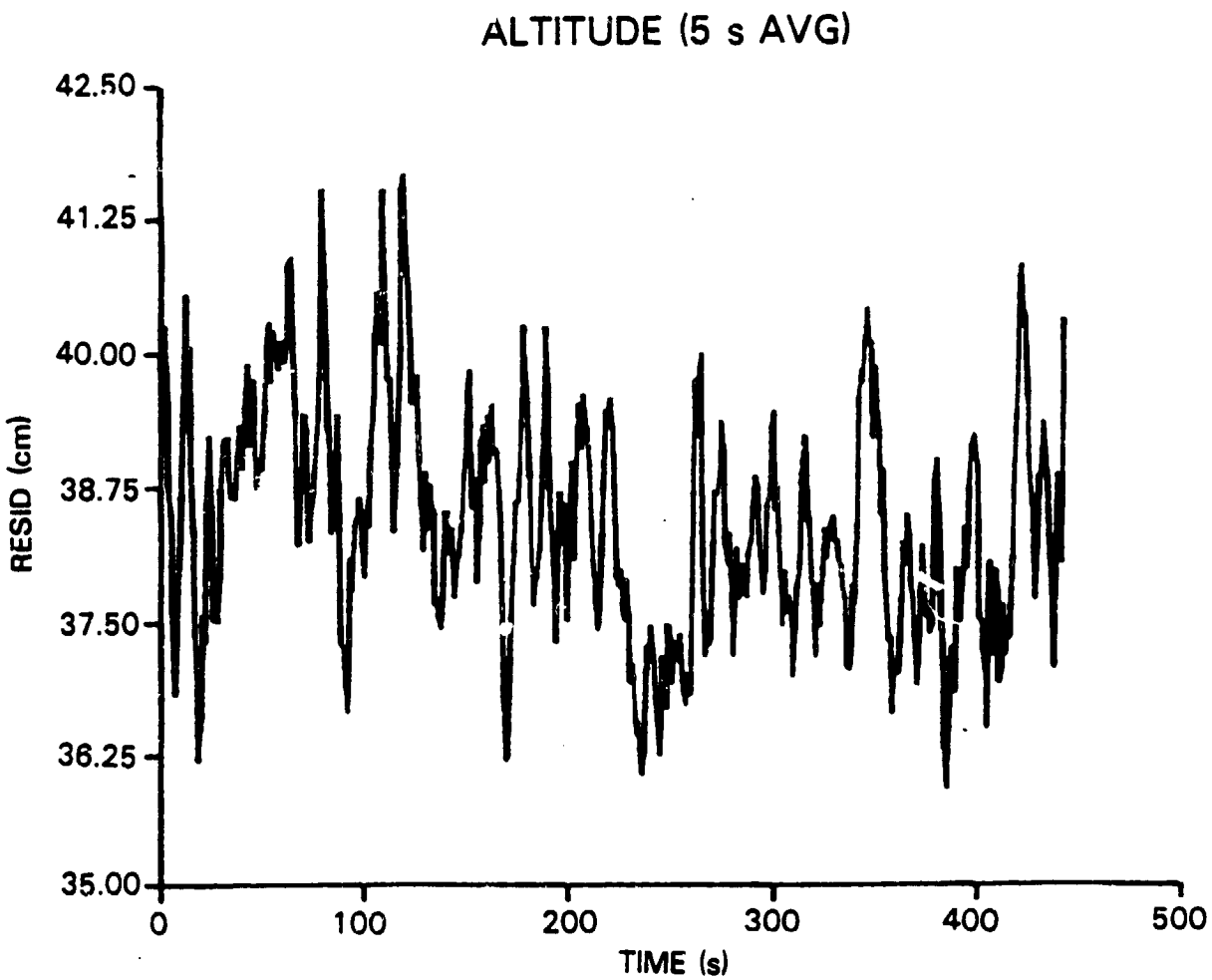

Fig. 11a — Altitude response to changes in AGC for 11-23-83

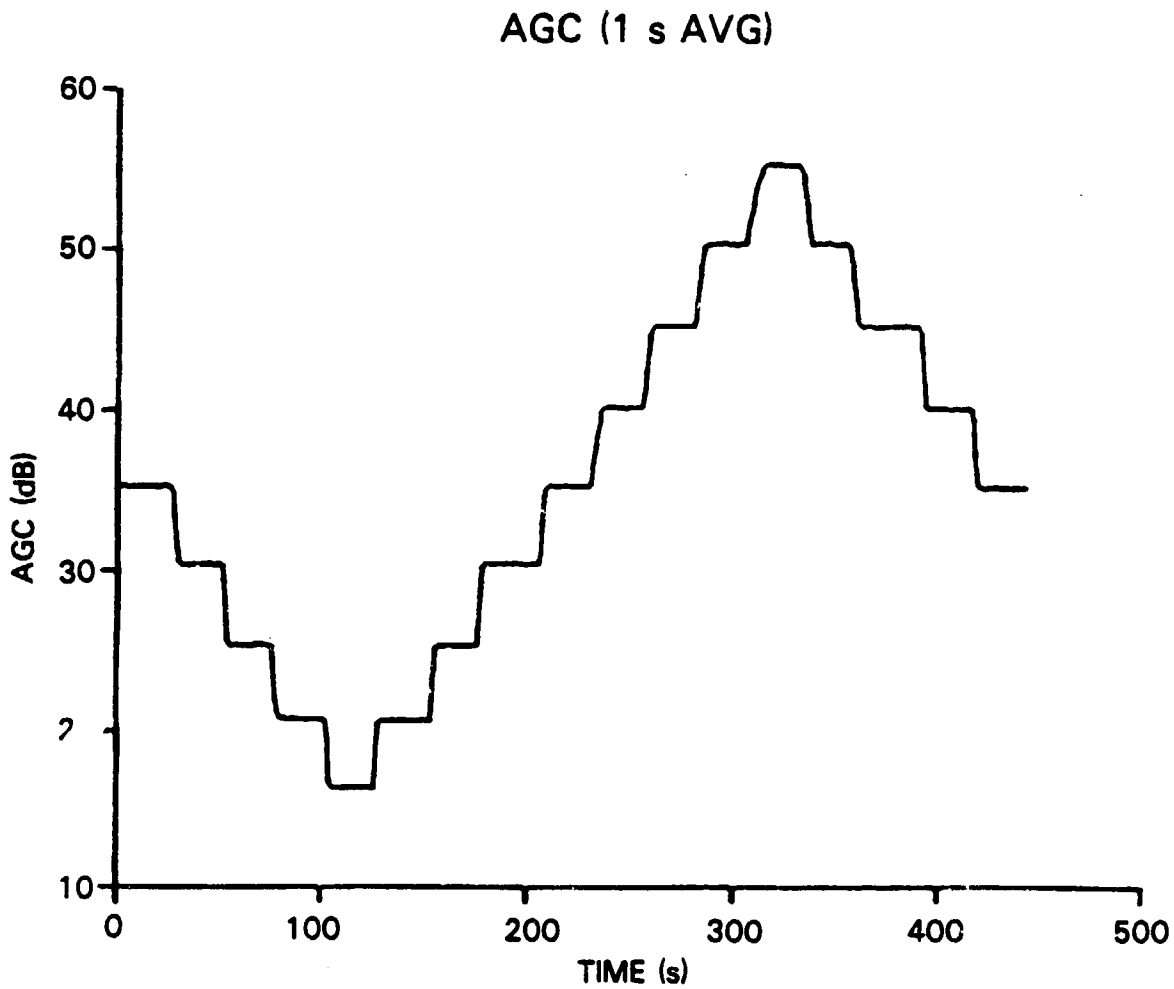

Fig. 11b — Altitude response to changes in AGC for 11-23-83

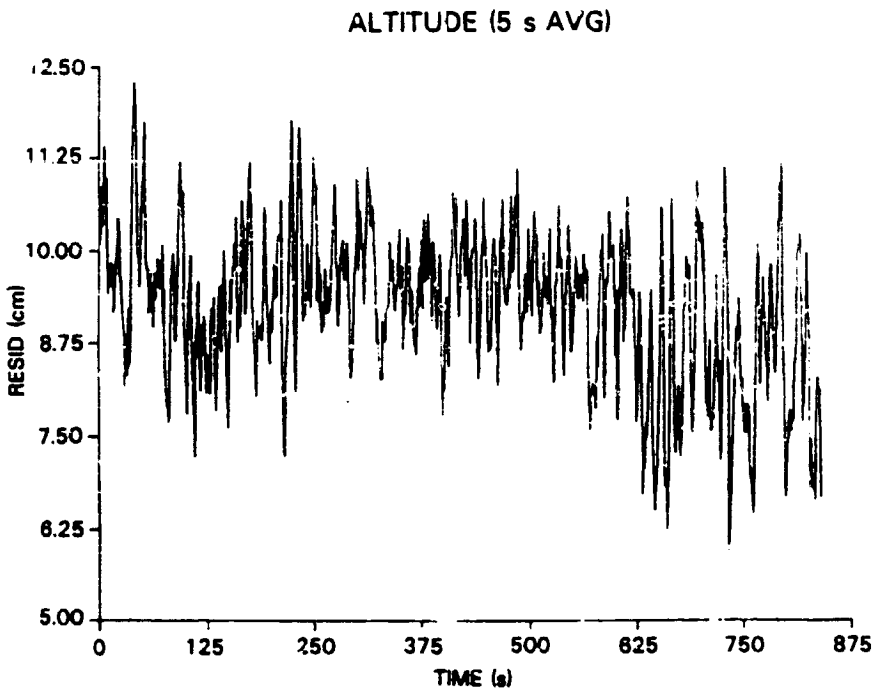

Fig. 12a — Altitude response to changes in AGC for 9-1-83 data

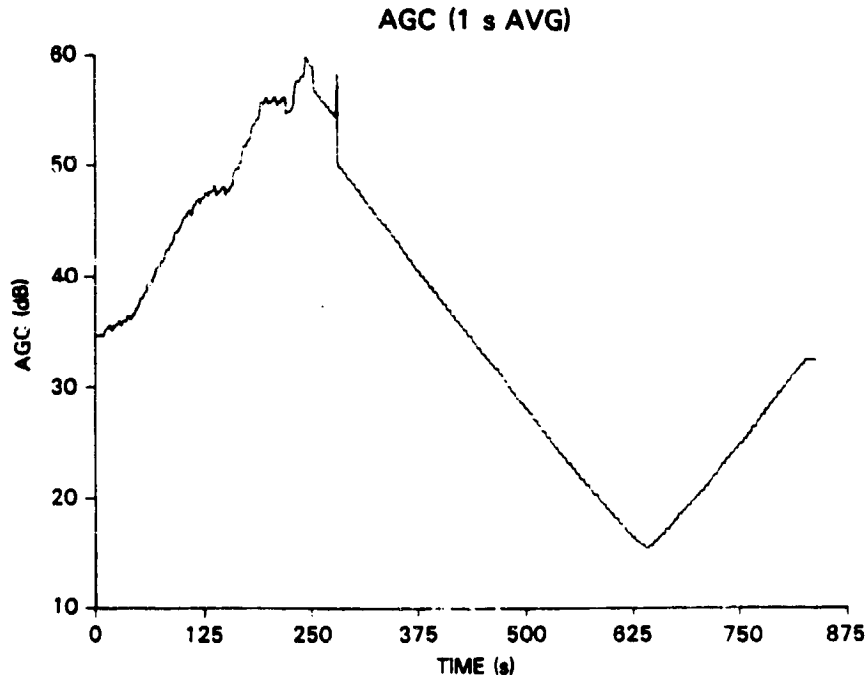

Fig. 12b — Altitude response to changes in AGC for 9-1-83 data

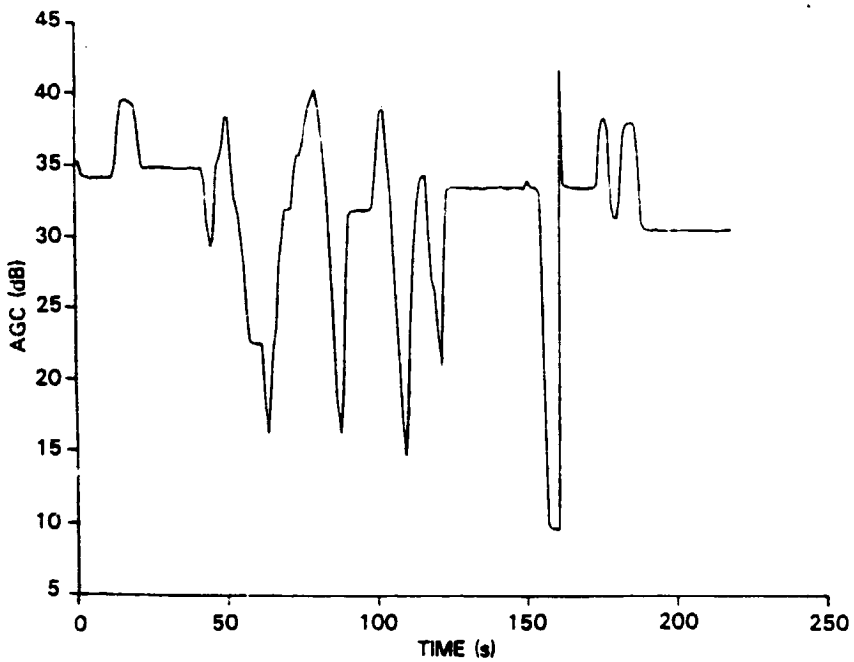

Fig. 13a — Manually inserted AGC changes made during test

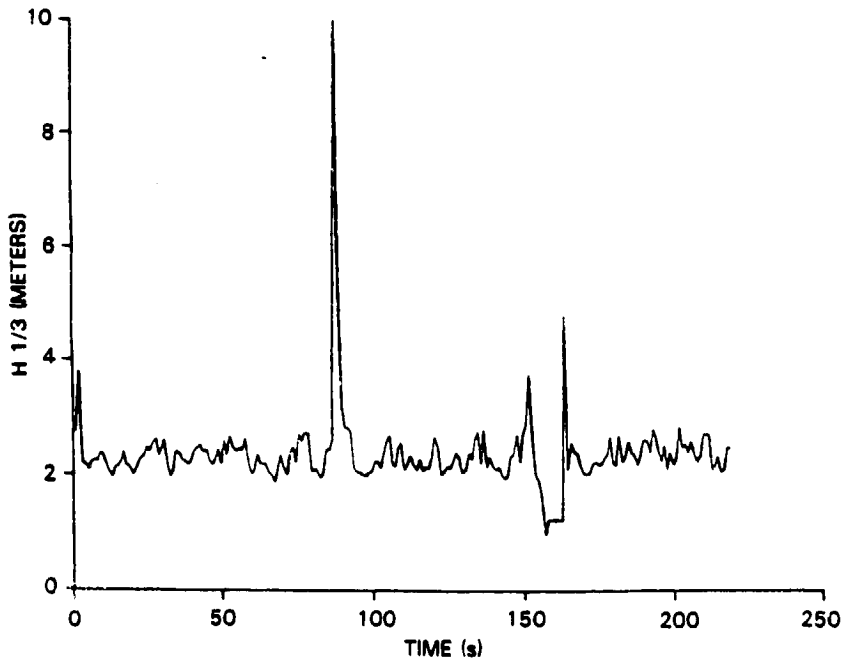

Fig. 13b — $H\frac{1}{3}$ response to AGC changes

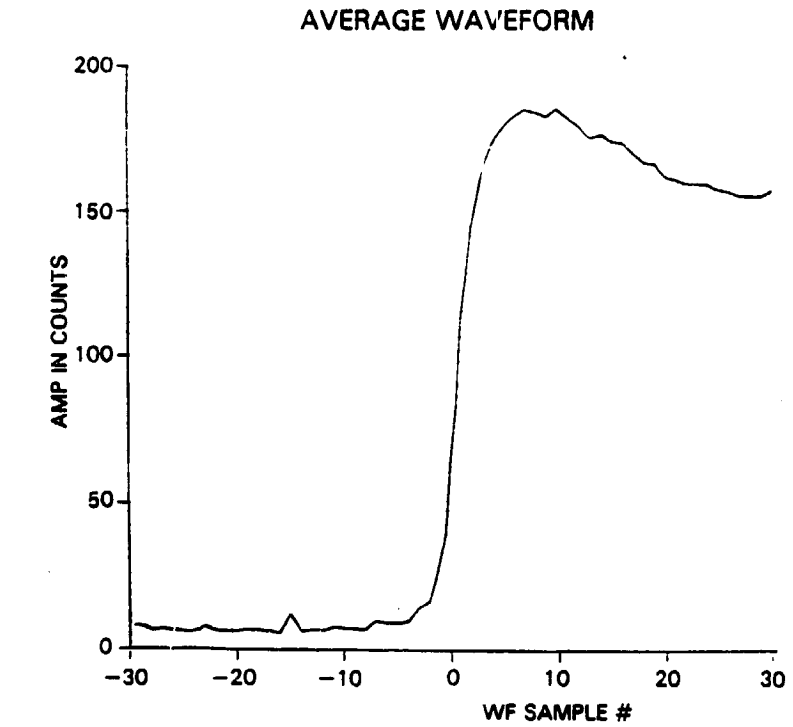

Fig. 14a — 36 second average waveform from 9-1-83 test, segment 1A,2B

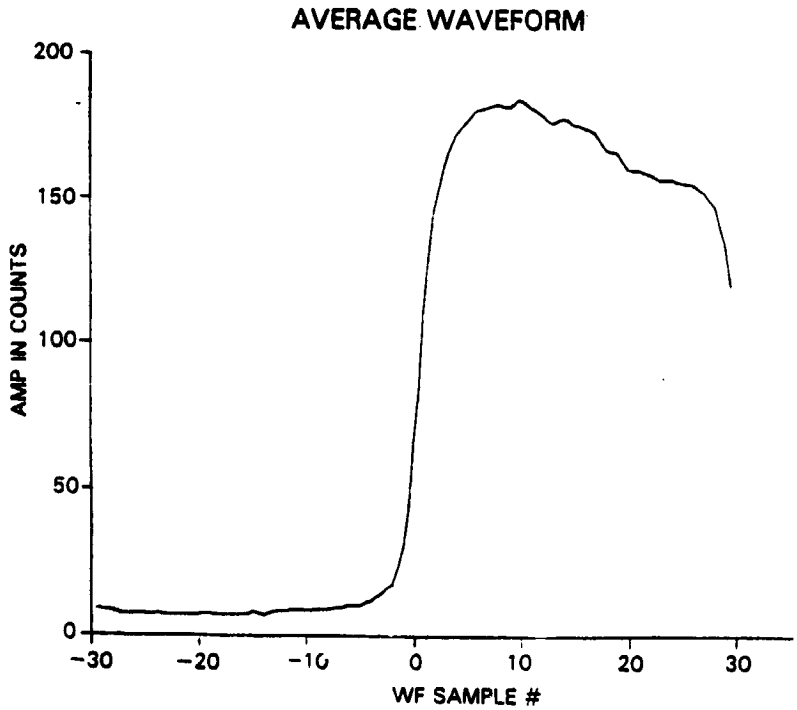

Fig. 14b — 36 second average waveform from 11-23-83 test, segment 1A,2B

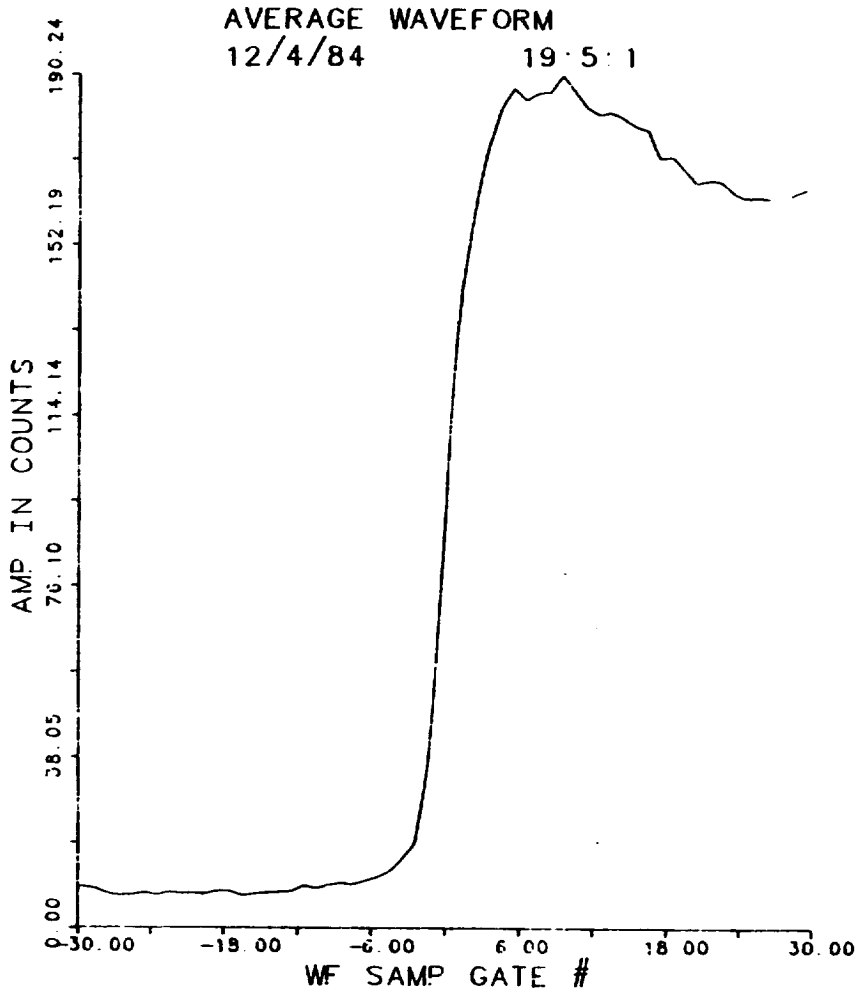

(a)

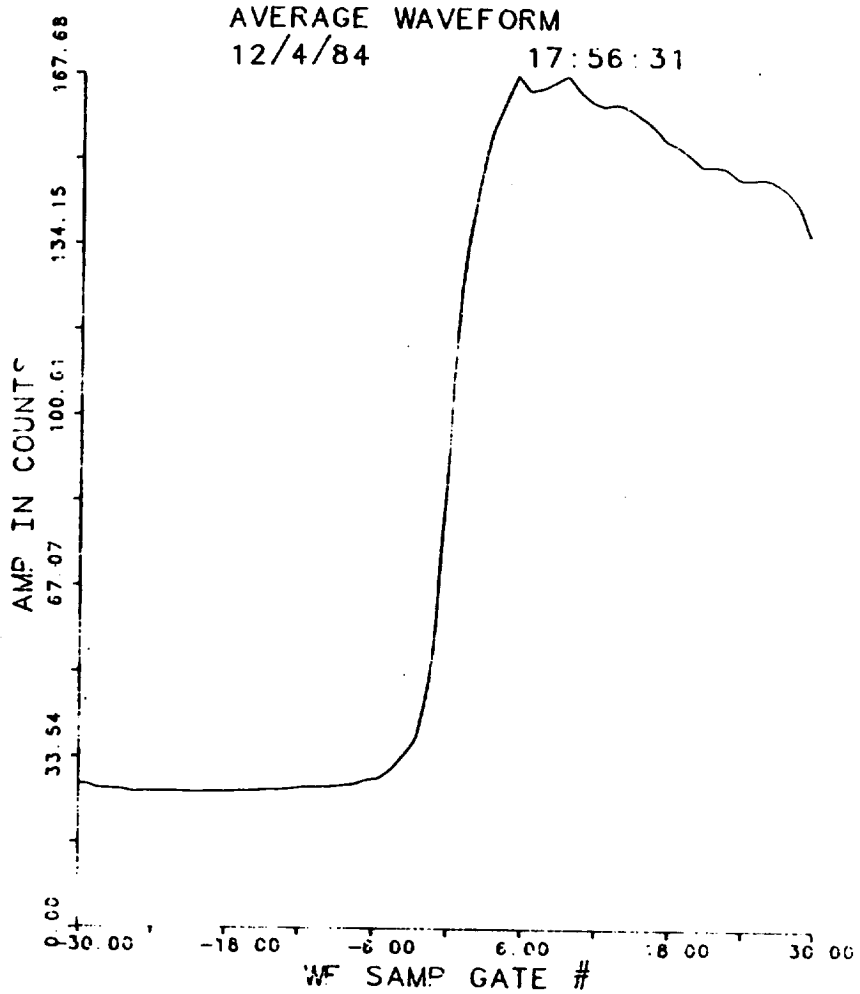

(b)

Fig. 15 — Waveforms recorded during 12-4-84

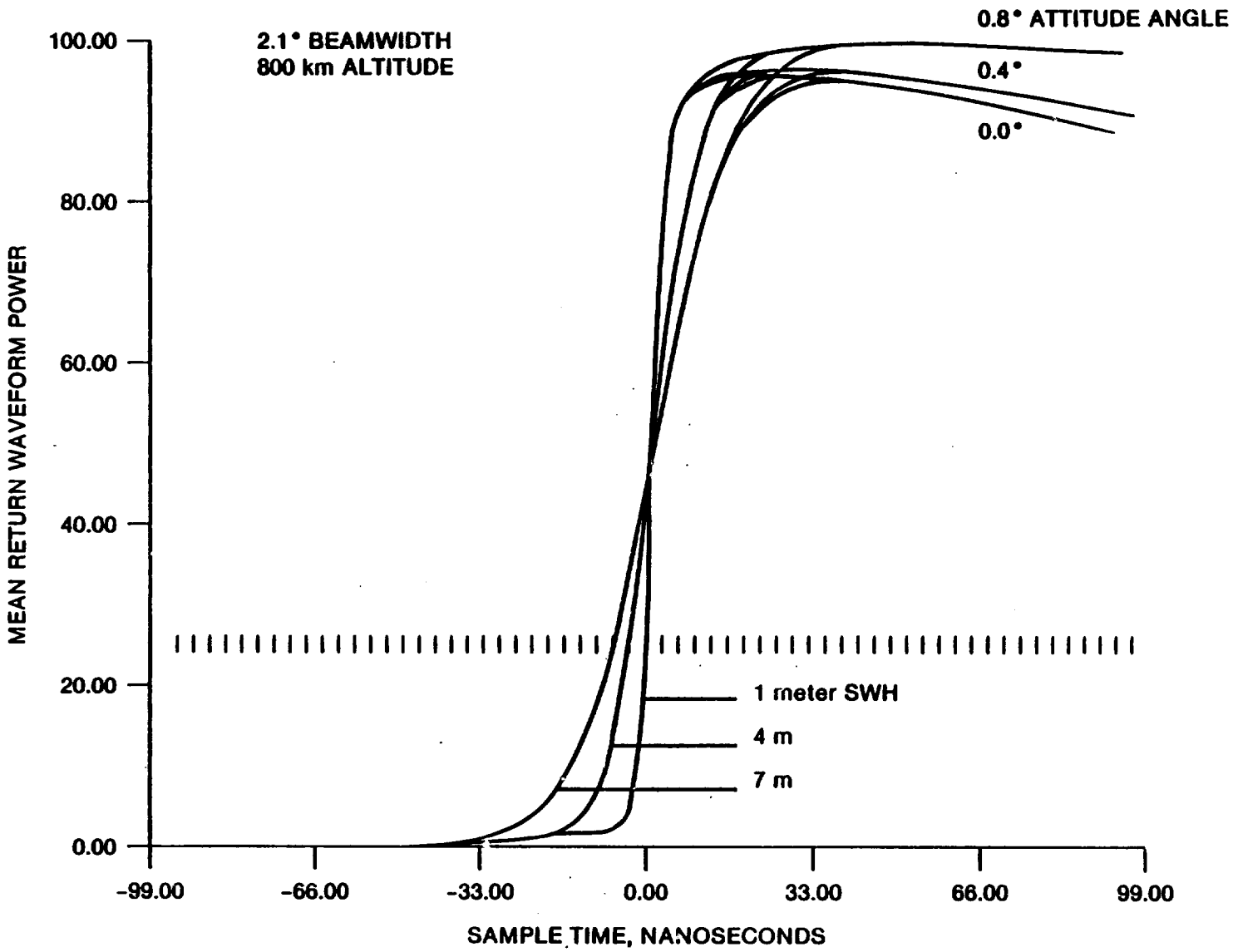

Fig. 16 — Mean return waveforms from a GEOSAT radar altimeter

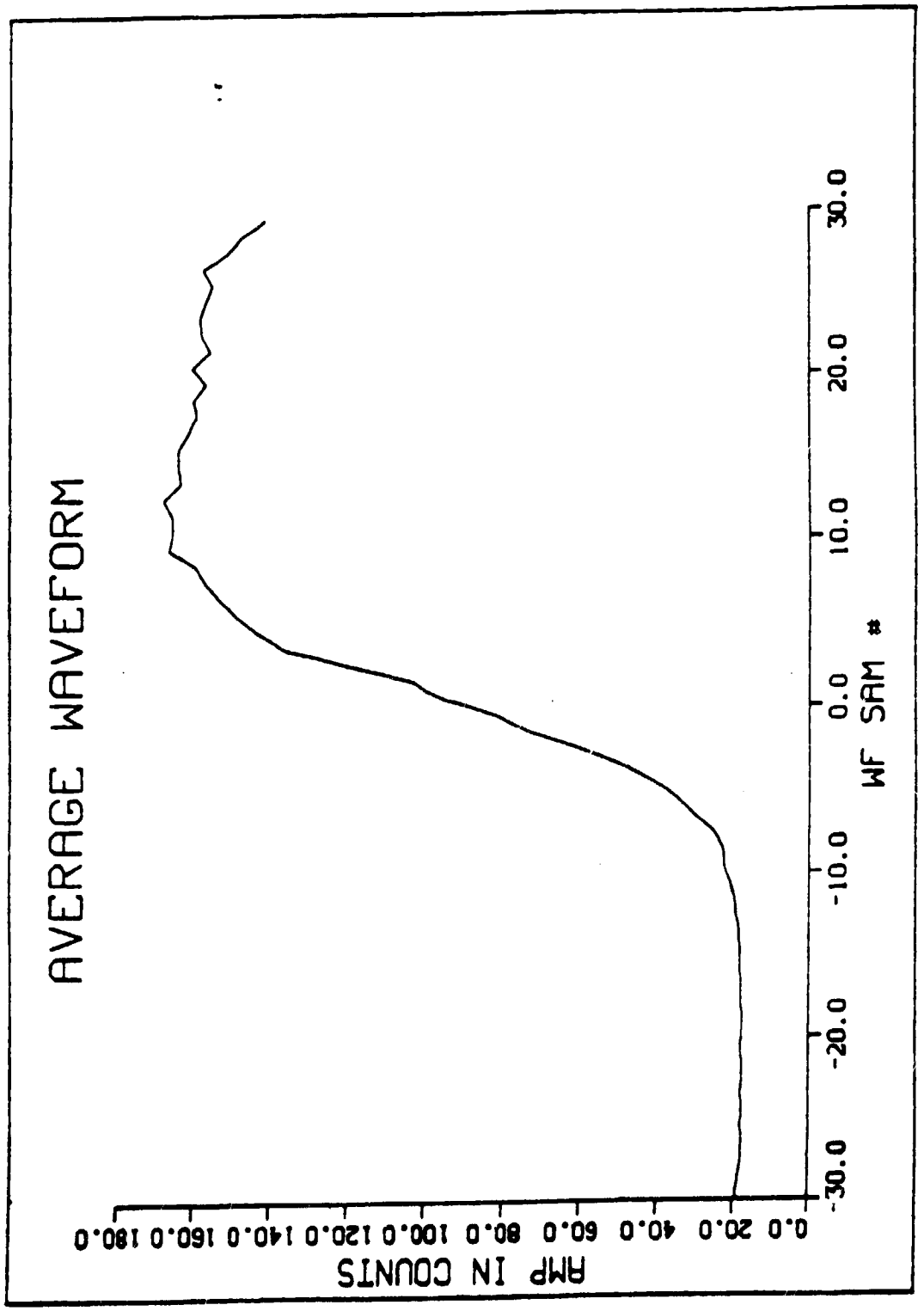

Fig. 17 — 36 second average waveform for 9-8-83 test, AGC = 19 dB, H $\left(\frac{1}{3}\right)$ = 8m

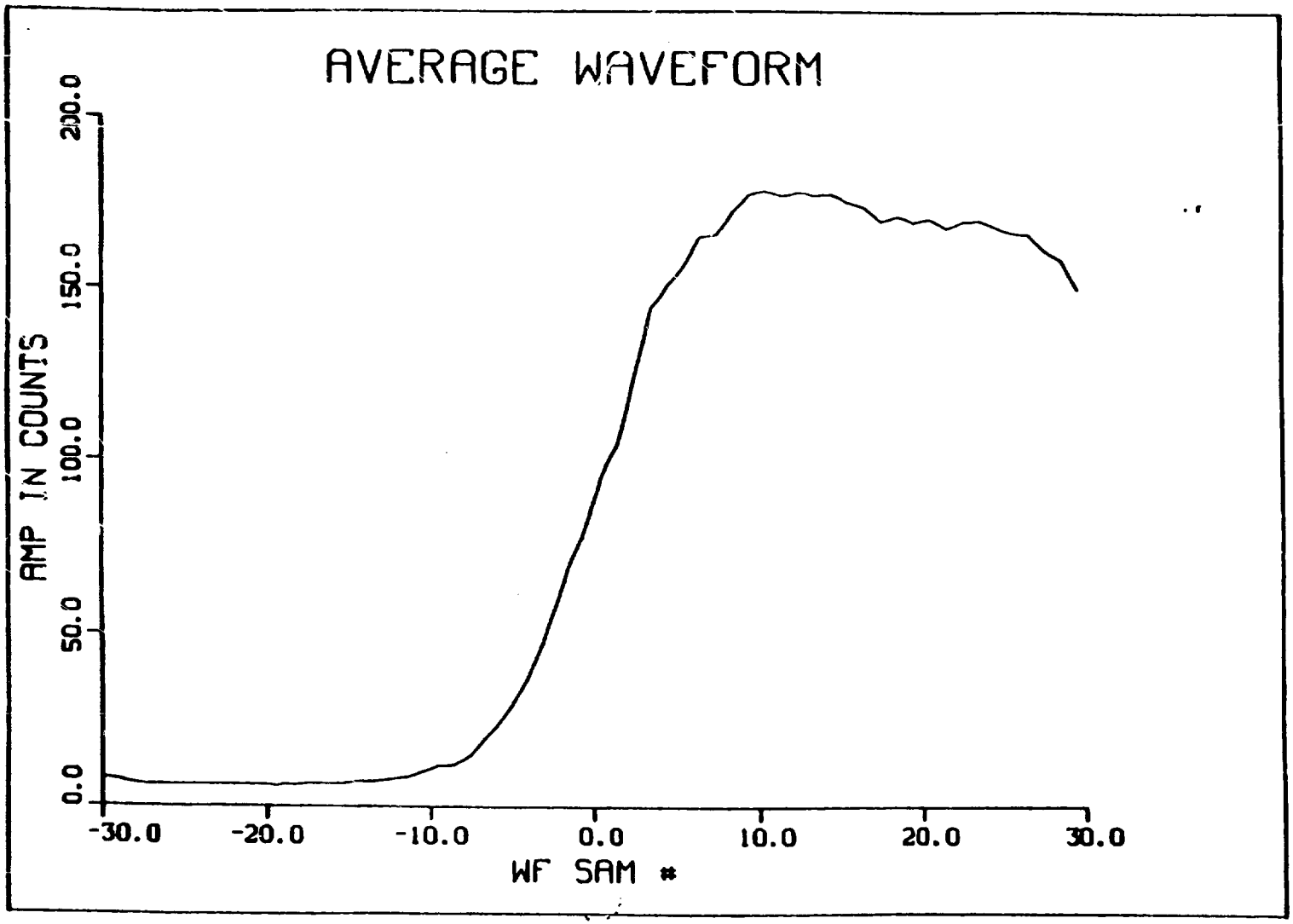

Fig. 18 — 36 second average waveform for 9-8-83 test, AGC = 37 dB, H $\left(\frac{1}{3}\right)$ = 8m

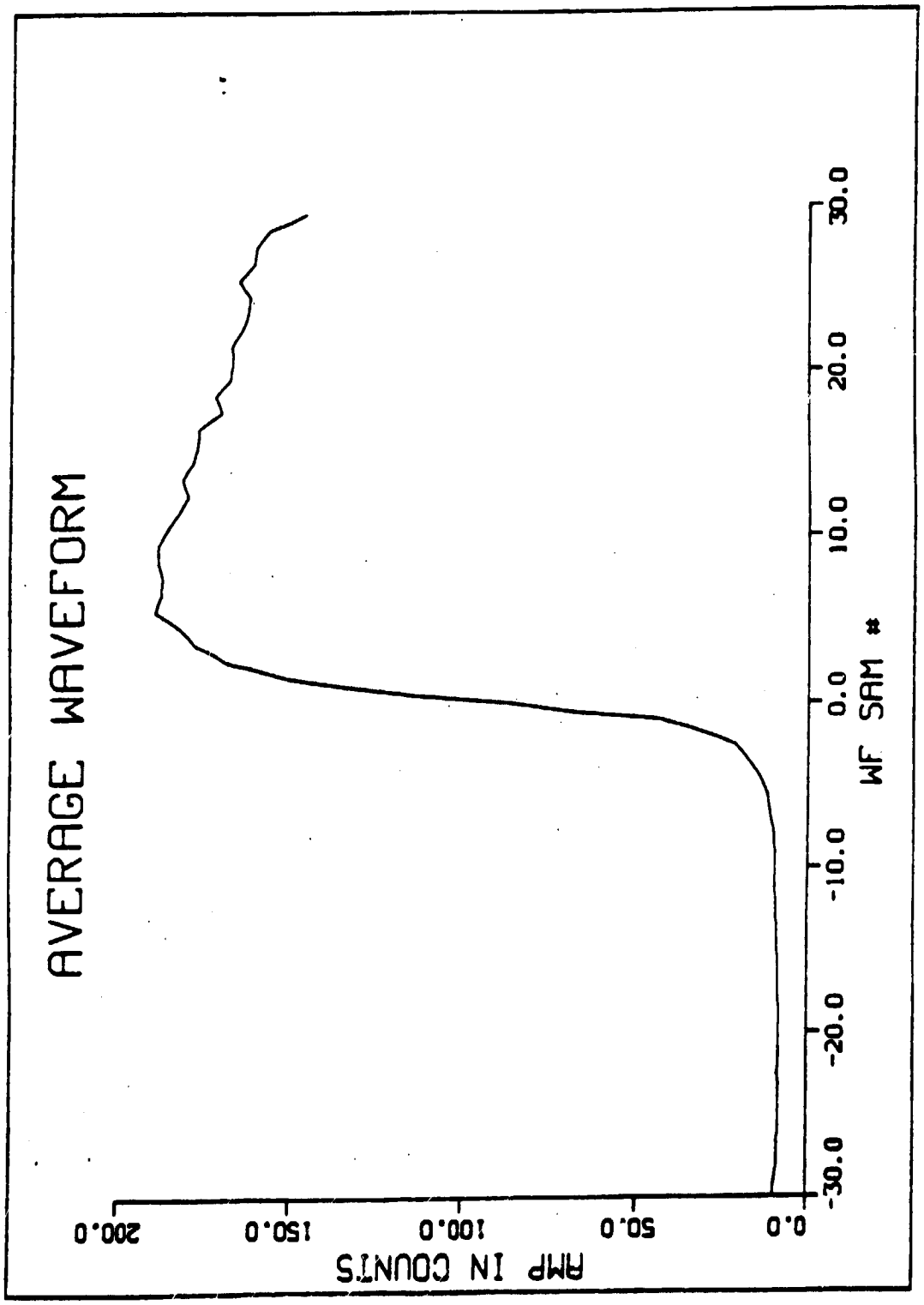

Fig. 19 — 36 second average waveform for 11-23-83 test, AGC = 25 dB, H $\left(\frac{1}{3}\right)$ = 2m

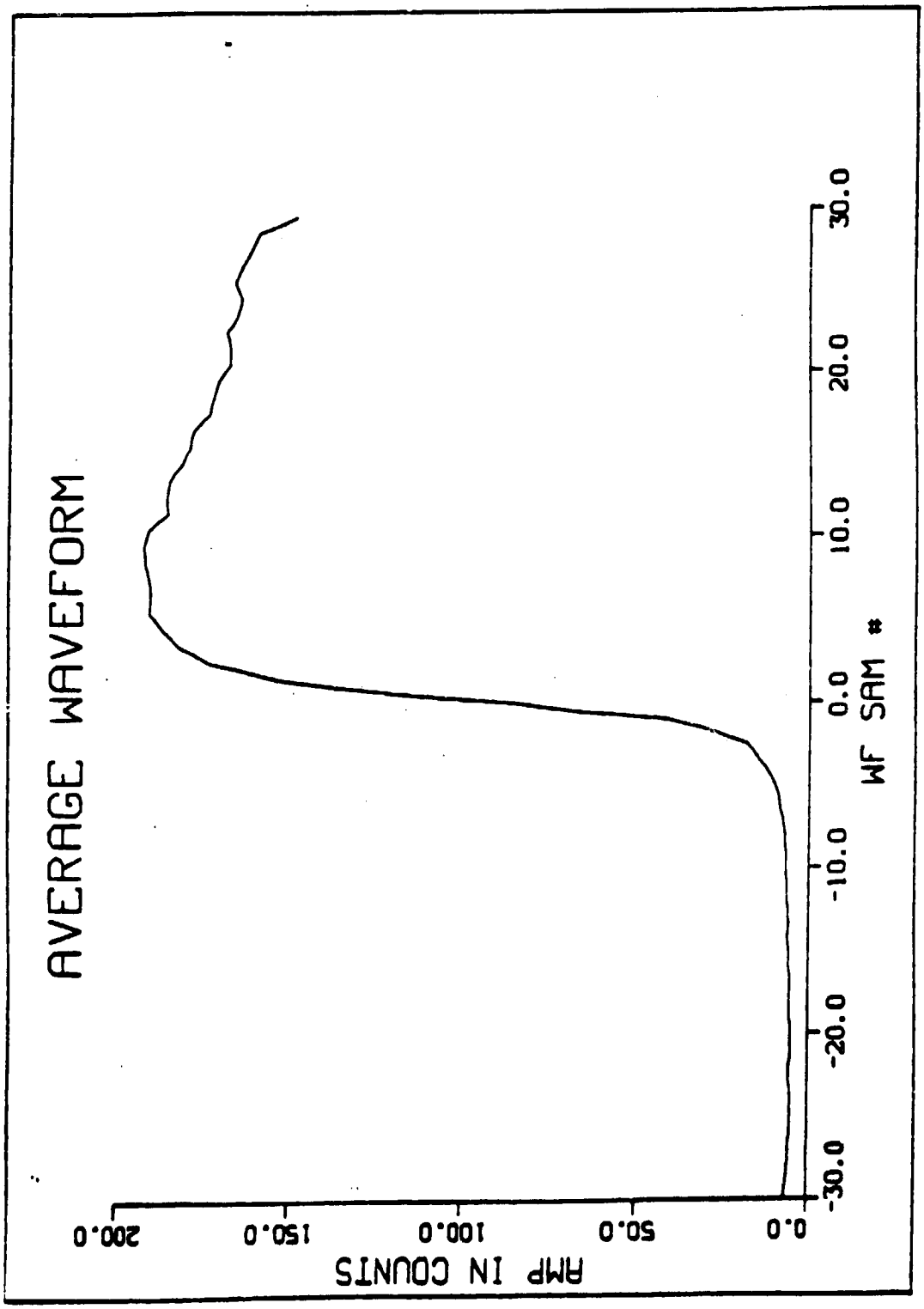

Fig. 20 — 36 second average waveform for 11-23-83 test, AGC = 44 dB, H $\left(\frac{1}{3}\right)$ = 2m

APPENDIX A

Pre-launch Test Sequence for the GEOSAT Altimeter

GEOSAT Special Tests

The tests were conducted under nominal conditions (i.e., 28 v d-c, altitude rate = 0 m/s, wave height = 2m). Conditions for 9-1-83 through 11-23-83 tests are listed below.

Test number	Special data products
1A tracker noise	Compute autocovariance function (ACF) and standard deviation (σ_h) on 10/s altitude data. Data acquisition period >3 min.
1B height correlation	Compute ACF and σ_h for altitude data and for 6 waveform samples which have first been averaged over 5, 10, 30 sec. periods. Data acquisition period ~30 min.
2A attitude estimation	Waveform and V_{AGC} values averaged over a 30 sec. period. Acquire 5 min. of test data, wait 5 min. and repeat test.
2B waveform correlation	Compute waveform sampler cross correlation for adjacent pairs i, i + 1 spaced pairs i, i + 2 spaced pairs i, i + 4 (i = sampler number, Δi = 3.125ns) (Only two waveform regions are of interest, the ramp midpoint and the plateau - correlation for all possible i values is not needed.)
3A Signal level effects	Record 1-sec. altitude average, wave height, and attitude angle versus AGC values of Hi, Nominal, and Lo.
3B Dynamic AGC effects	Repeat 3A with Hi AGC and with signal level changes made manually using a waveguide attenuator installed between RASE and altimeter to test system under dynamic AGC conditions. Changes should span ~25 dB, but not to the point of break-lock.
3C Dynamic AGC effects	Repeat 3B using gradually increasing, then decreasing values of attenuation in ~0.5 dB steps to exhibit AGC resolution characteristics.

Test schedule for 12-4-84 activity.

(All times below are approximate only)

TAPE #	SEG I	TIME hh:mm:ss	TEST ACTIVITY
F301	A	17:08	Calibration, after starting in Track 1
	B	17:10	End calibration
	C	17:11:30	Start long track segment, nominal 2m SWH, zero h-rate
	D	17:44	Start calibration
	E	17:46	End calibration
F302	A	17:55:30	Start low SNR, zero h-rate segment, 2m SWH
	B	17:56:30	Set h-rate to 25m/sec, otherwise same as above
	C	18:06:30	Change to 8m SWH, otherwise same as above
	D	18:16:30	Change to higher SNR, otherwise same as above
	E	18:26:30	Change to 2m SWH, otherwise same as above
	F	18:34	End of tape, abort & rewind
F303	A	18:39:40	NRL special test sequence, abort after 1st 8m SWH case
	B	19:02:50	Put in steady track, zero h-rate
	C	19:03:20	Increase height by 50ns from above
	D	19:03:40	Remove above 50ns height step, back to 0 height offset
	E	19:05:00	Make series of short 10 dB changes in SNR, up or down
	F	19:06:20	Start ramp of 5 dB steps in SNR, 20 sec. each step
	G	19:12:33	End of AGC test, end of this tape's data

... above this point the Adaptive Tracker Unit (ATU) #1 was used ...

... below this point, the ATU #2 was used ...

F304	A	19:25:00	Calibration
	B	19:17	End calibration
	C	19:27:33	Start stable track
	D	19:37:00	Step 50 ns in height
	E	19:37:20	Return to zero height offset Begin set of AGC changes by 10 dB steps
	F	19:38:40	Start ramp of 5 dB steps, 20 seconds per step
	G	19:44:20	End 5 dB step sequence
	H	19:45	"Dynamic ocean" manual, random AGC changes
	I	19:47:40	Calibration
	J	19:50	Finished

APPENDIX B

The calibration mode data for the GEOSAT radar altimeter from thermal vacuum testing from 10/29/83 to 11/01/83 have been analyzed for temperature effects. The results showed that the height was nearly insensitive to temperature variations, but the AGC required correction. The analysis used six of the 11 steps (steps 12 dB to 42 dB each separated by 6 dB) because the other steps showed system differences. The six steps used covered the normal range of operations. The power in the zero gate for all 11 steps for one calibration is shown in Figure B1 and indicates that steps <12 dB and >42 dB responded differently. The Calibrated mode height for one calibration for the six selected steps appears in Figure B2. This showed a maximum height difference of 0.01ns (0.15cm) between the steps and indicated that there was no height bias correction needed for AGC changes.

The receiver temperature profile for the set of calibrations used is shown in Figure B3. The height dependence on receiver temperature was 0.0013ns/^{o}C (0.02cm/^{o}C) and typical data are shown in Figure B4. This indicates about 1cm of change for a 50^{o}C range and can be ignored for GEOSAT. The calibration step for 36 dB was chosen for a typical example of the calibration mode response. The other steps have been analyzed and respond similarly.

A linear fit of AGC to receiver temperature was made for each of the six steps. The slopes were nearly identical and therefore the mean slope of 0.1185 dB/^{o}C was used as the temperature correction for AGC. Typical AGC dependence versus receiver temperature is shown in Figure B5. The data were also analyzed against the Microwave Transmission Unit (MTU) temperature, but no trends were noticed between AGC and MTU temperatures. It can also be seen that the data taken during temperature transition ("on the fly") do not align with the data taken after a temperature soak. This is interrupted as a temperature detection verses stabilization error and not a requirement to fit the data with a quadratic. It is recommended that at least one soak at a mid-temperature be done in future altimeter testing. The transmit power was also analyzed and was found to decrease with a MTU temperature increase. The typical data are shown in Figure B6.

As a test of the AGC temperature correction, the AGC from the 30 minute stable track on 9/1/83 was temperature corrected. The AGC before correction is shown in Figure B7, and after correction is shown in Figure B8. The results appear to be excellent and yielded a standard deviation from the mean of one second averages of 0.05 dB after the temperature correction was applied.

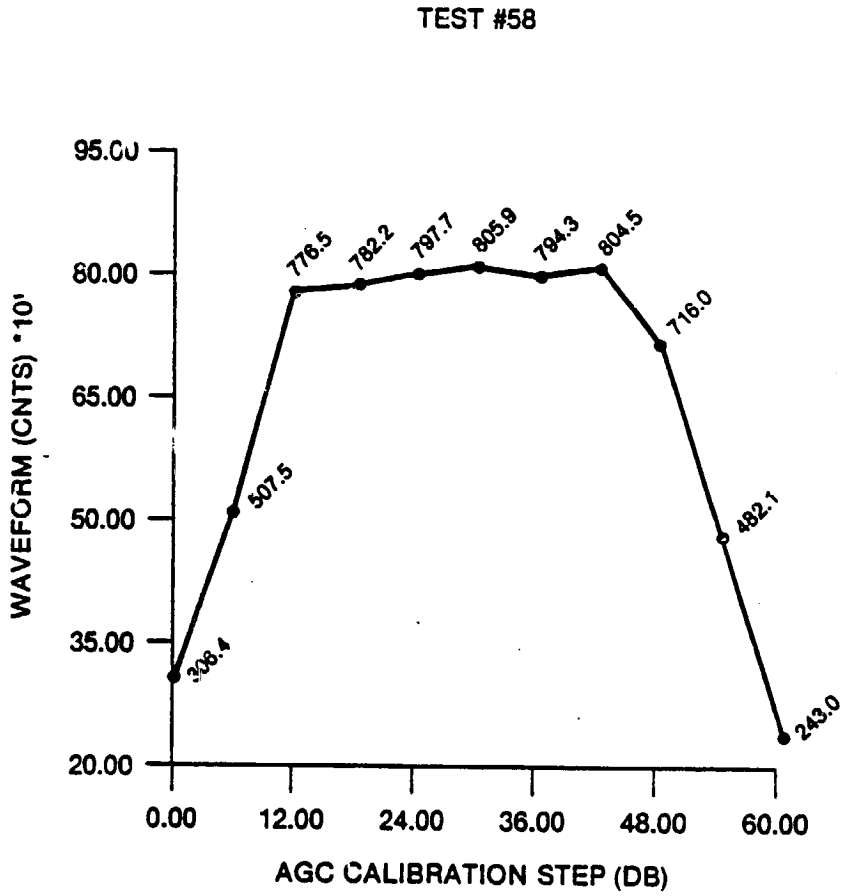

Fig. B1 — Waveform sample 0 for each calibration step

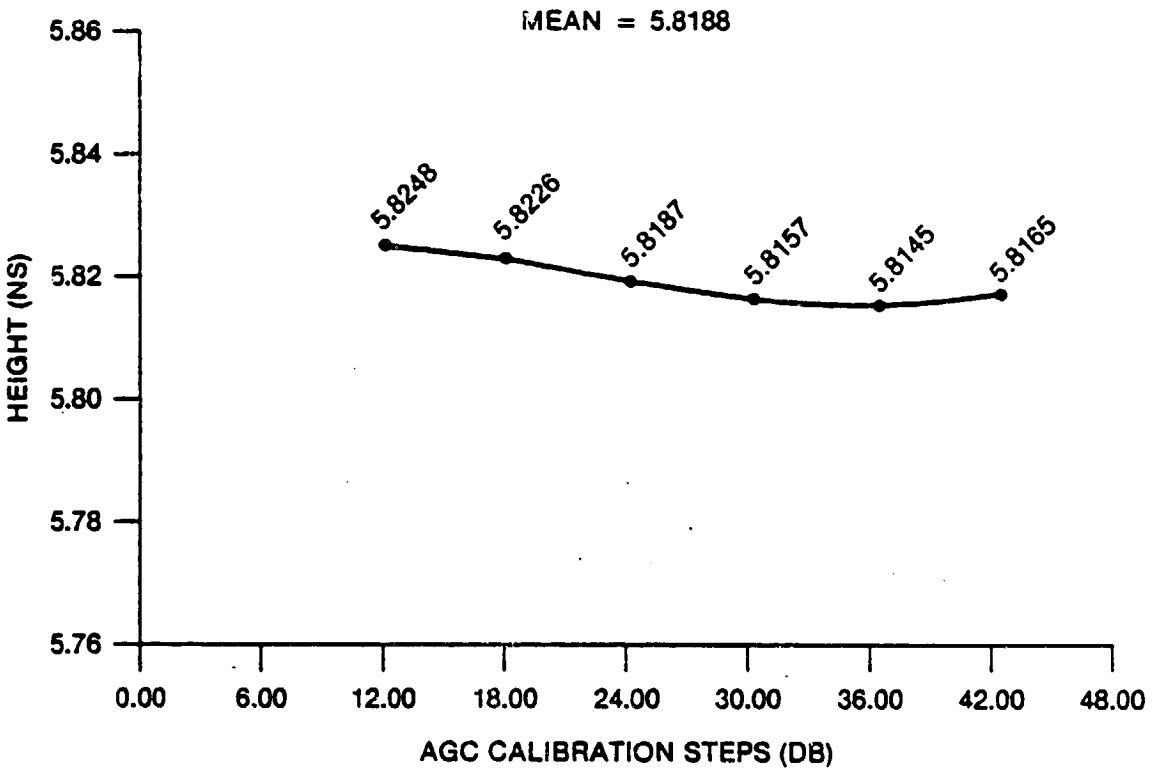

Fig. B2 — Calibration mode height for six steps used

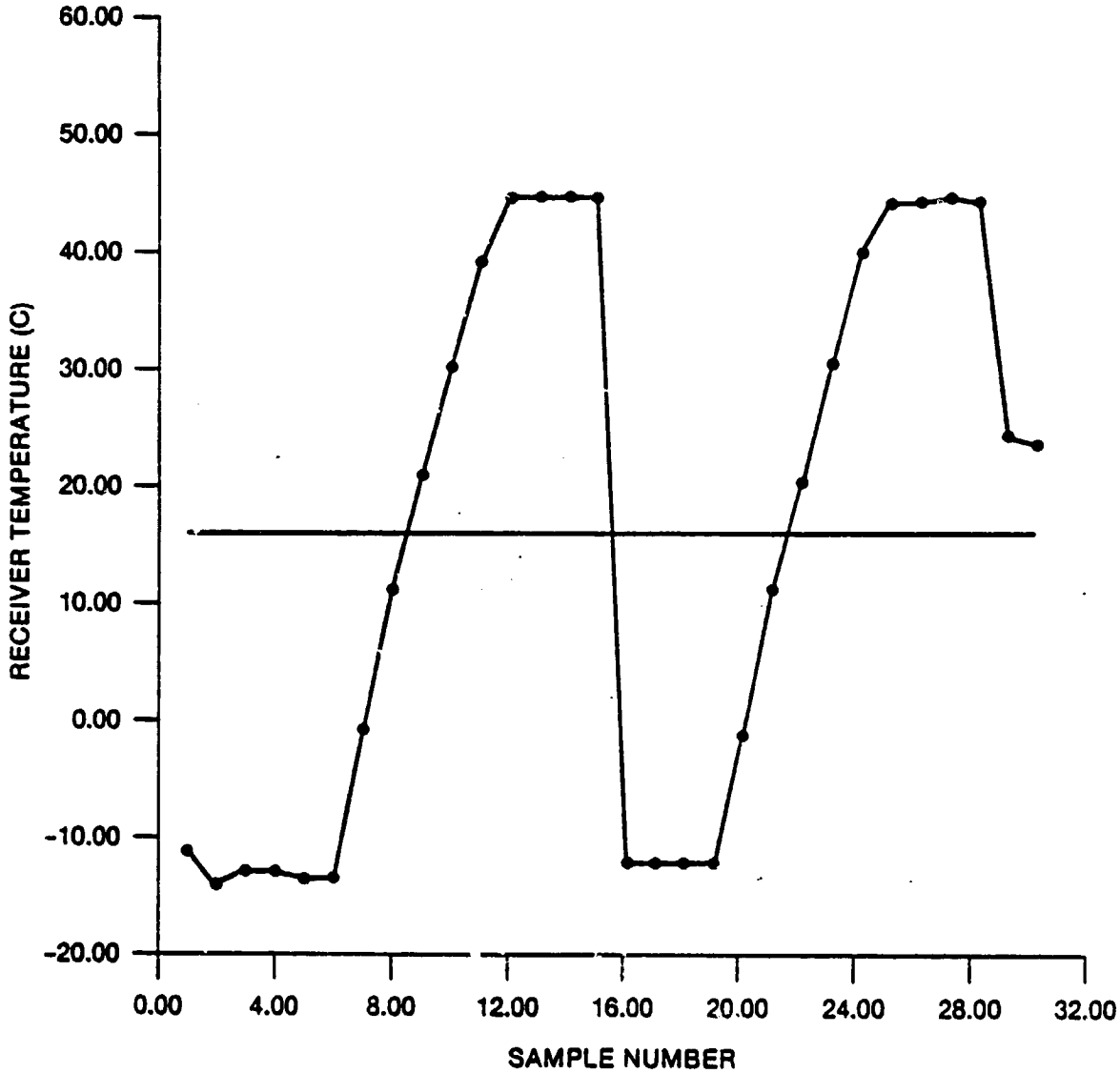

Fig. B3 — Receiv.. temperature profile

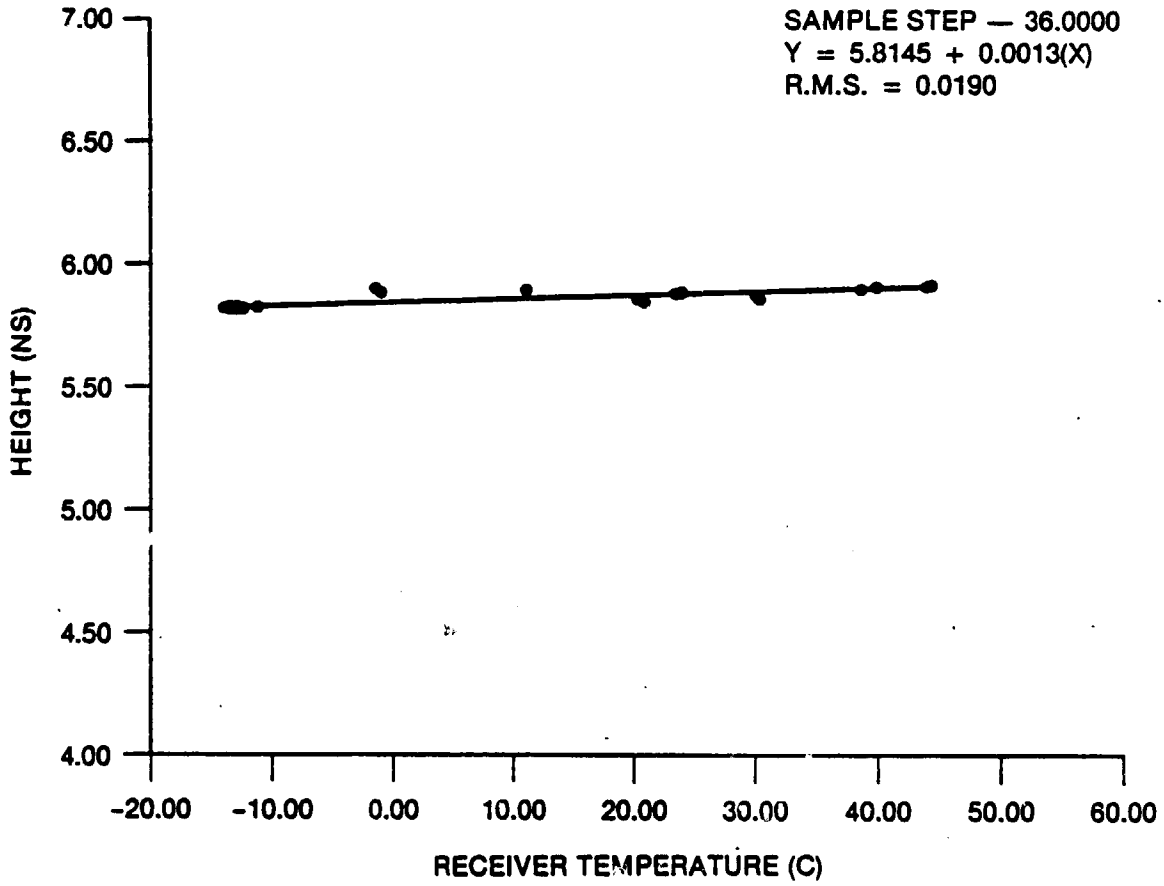

Fig. B4 — Calibration mode height as a function of receiver temperature

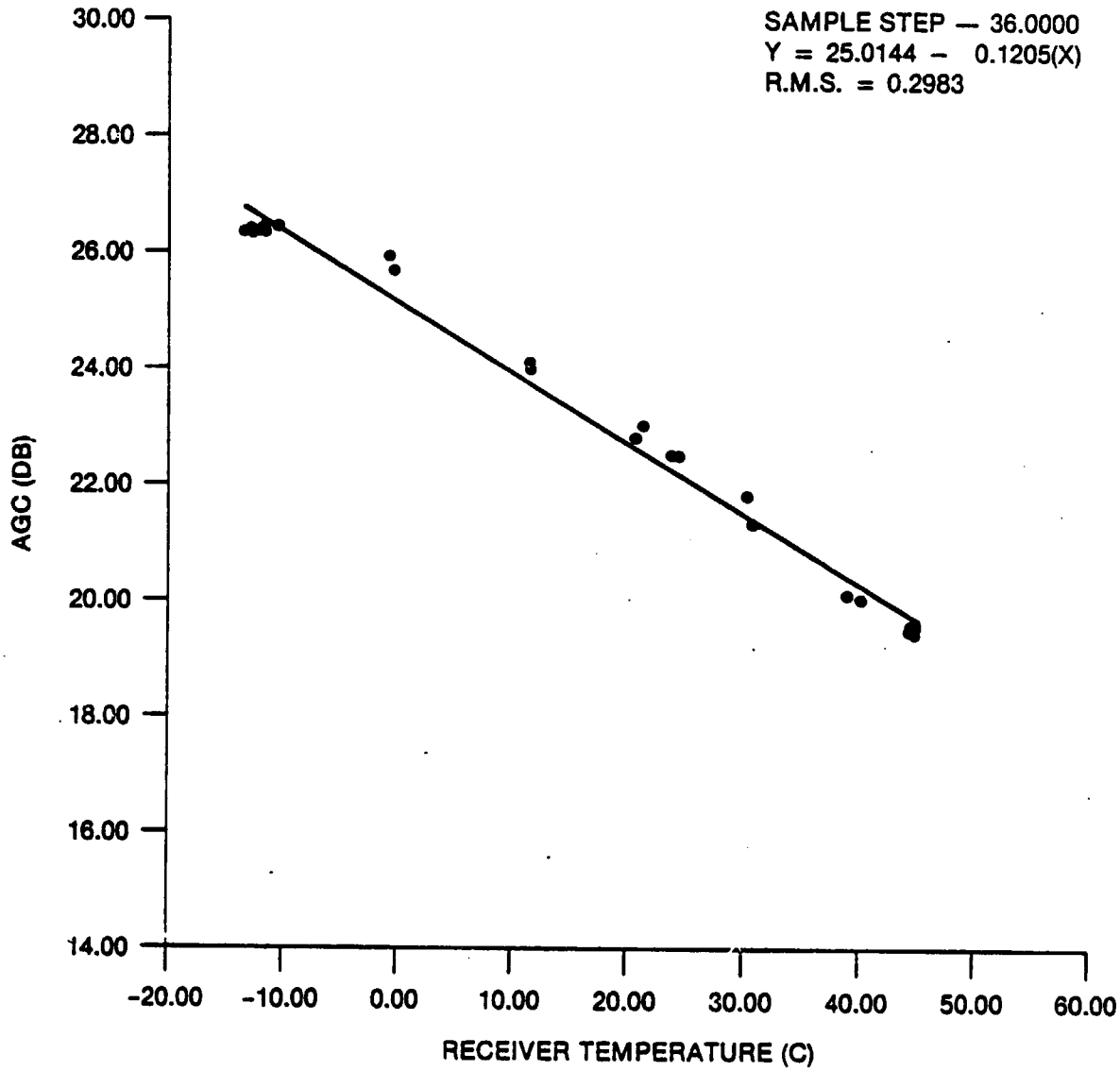

Fig. B5 — AGC as a function of receiver temperature

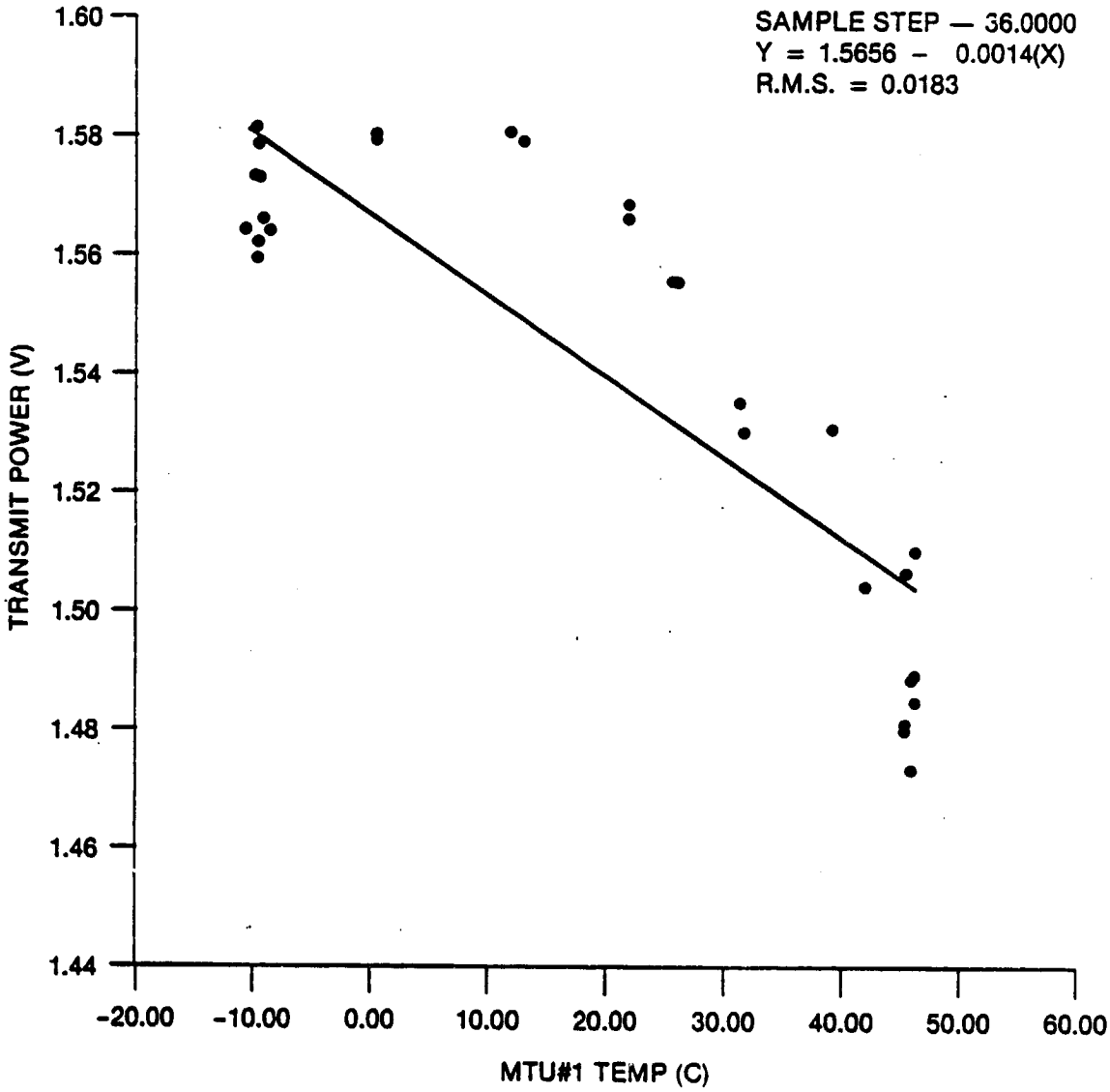

Fig. B6 — Transmit power as a function of MTU temperature

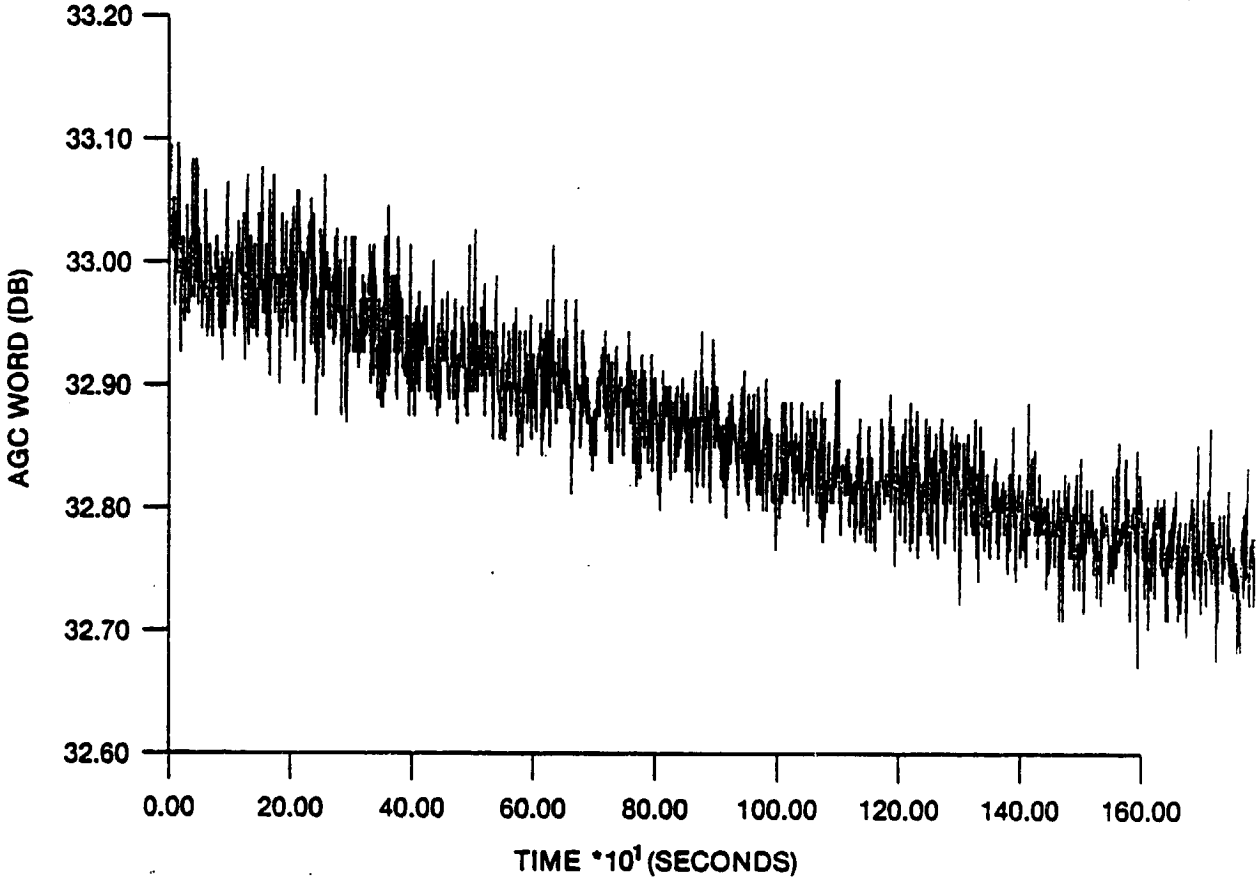

Fig. B7 — AGC during 9/1/83 long track

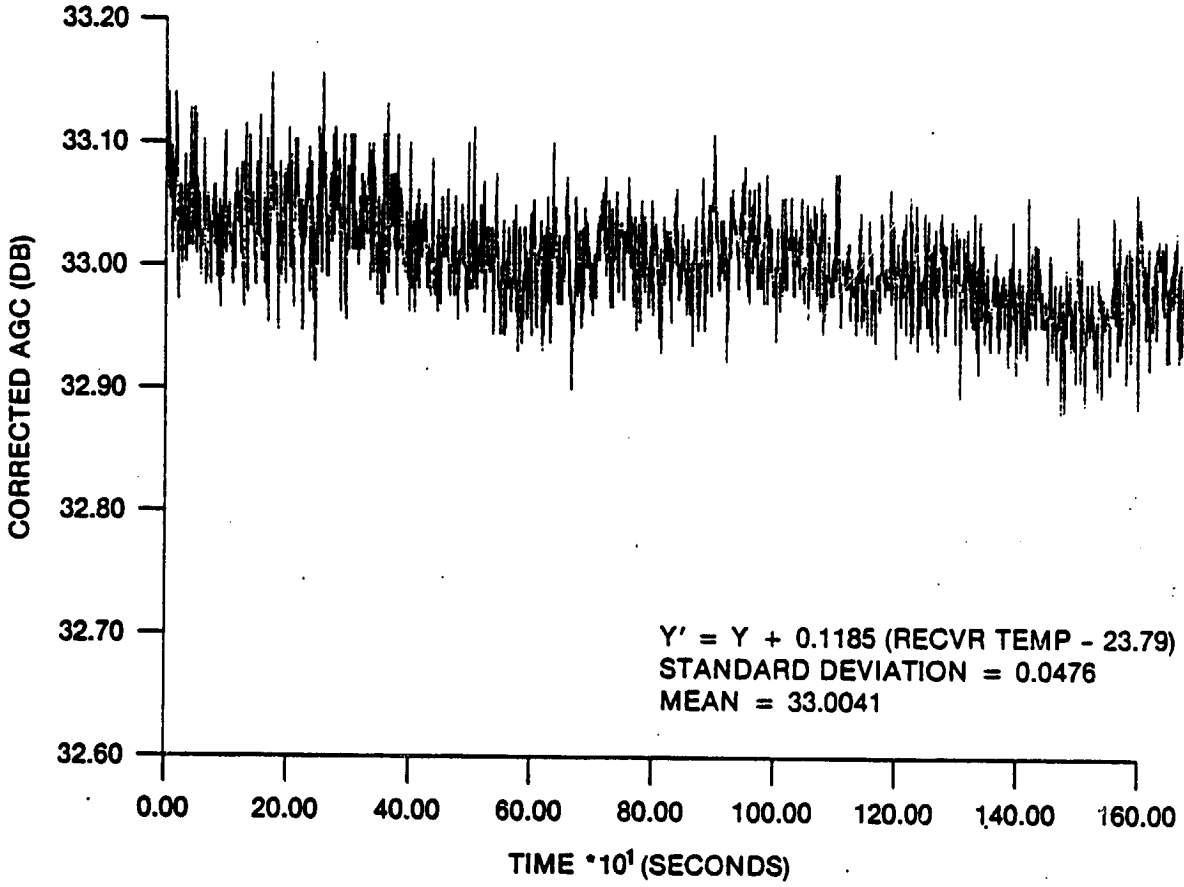

Fig. B8 — AGC corrected for receiver temperature during 9/1/83 long track

APPENDIX C

AGC Data Analysis from Special Test 3C

In GEOSAT Special Test 3C, a series of signal level changes were made using an analog attenuator installed between the RASE and the altimeter. The attenuation was changed in 0.5 dB steps and, because the output data record could not show when the attenuator was changed, the step-changes in attenuation were manually set every 5 seconds. Making these attenuation changes uniformly in time allowed the examination of the linearity of the altimeter's AGC response even though the exact setting of the attenuator was not known and the time of each AGC step was never explicitly recorded.

The test sequence was started with the altimeter AGC in about the middle of its range. The attenuator was decreased in 0.5 dB steps over a 20 dB range, then increased in 0.5 dB steps over a 40 dB range to a value 20 dB greater than the starting point, and finally decreased again by 0.5 dB over the 20 dB range to bring the system back to the original starting point.

Part of the AGC data versus time from this test sequence from GEOSAT tests run on test date I are shown in Figure C-1. The value of the AGC vs. time was a series of noisy steps. The leading edge of each step was unreliable since it contained the human operator's finite setting time for each new attenuator setting as well as the AGC settling time, but the latter part of each step should be a reliable estimate of the steady-state AGC value which the altimeter produced.

The analysis of the results of Test 3C data required more manual analysis, also indicated in Figure C-1. A horizontal pencil line (not shown) was drawn at each AGC step to represent the eyeball-selected best estimate for the value of the latter half of each step. A ruler was then used to measure the distance from the horizontal axis to the step, and the series of values so obtained were entered in Table C-1 (measured from edge in 1/60 in.). The ruler-measured distance values (using the 60 divisions/inch scale on an engineering ruler) were then converted to the AGC values given in the third column of Table C-1 (calculated AGC, in dB).

Incidentally, there was one obvious operator error discovered in the data of Figure C-1: the 22nd attenuator change in the sequence was obviously 1 dB instead of the 0.5 dB. On the later segment when the AGC was decreased, the correct 0.5 dB change was made in coming back down through this value, and the system AGC measurement showed the correct steps of the order of 0.5 dB. One false data point has been inserted in Table C-1, at the 22nd entry, to show the 32.0 dB AGC which presumably would have resulted from the correct attenuator value. The value at 32.0 dB was obtained by linear interpolation between the values 31.5 and 32.5 dB.

A set of "absolute" step numbers was then assigned. The lowest AGC output (from the highest external attenuation) was arbitrarily assigned the value 1. This is the 128th entry in Table C-1. The next higher AGC output, both before and after this lowest value, was assigned the value 2 (at the 127th and 129th values in Table C-1). This process was continued, with the result that the highest AGC value (from the lowest external attenuation)

became absolute step #81 (see the 48th entry in Table C-1). This set of absolute numbers is listed in the fourth column of Table C-1 under the heading "New Change #".

If the altimeter performed a perfect, error-free power measurement, its AGC output would be a straight-line function of the absolute step number from Table C-1, fourth column. This step number was designated as n and, using the first entry from Table C-1, 30.6 dB at n of 34, and the knowledge that the straight line slope has to be 0.5 dB per step, the straight-line relationship is

$$AGC = 30.6 + 0.5 * (n - 34)$$

where AGC is in dB. This value is given as linear AGC of Table C-1, and the residuals, the differences between the output AGC (column 3) and the linear AGC are shown in the last column (calculated AGC minus linear AGC). These residual values, in dB, are a direct indication of the relative accuracy of the AGC measurement. Notice that these values are typically 0.1 to 0.2 dB either side of 0, and vary relatively randomly. The graphical extraction of data from Figure C-1 to produce the values in Table C-1 is itself no better than 0.1 dB.

Figures C-2 to C-4 show some of the information just discussed. First, Figure C-2 shows the altimeter AGC vs. the manual change step number, columns 3 vs. 1 of Table C-1, and the overall sequence (up 20 dB, down 40 dB, up 20 dB) of Test 30 is seen. Figure C-3 then shows these same AGC data, but this time they are plotted vs. the absolute step number, n, of column 4 in Table C-1. Finally, Figure C-4 shows the AGC residuals of column 6 in Table C-1 as a function of the column 4 absolute step number, n. The different plot symbols in Figure C-4 are in the test order: the squares start at the middle of the range and move up in step number, n, from the start of the test through the initial 20 dB decrease in the external attenuator, then the "+" symbols cover the middle of the test with the 40 dB attenuation increase, finally the dots indicate the last 20 dB change in the test sequence. Notice the departure from linearity of the AGC output for low AGC value, as shown by the larger residuals in Figure C-4 below the AGC step number, n, of 20. This is an expected result since at lower values of signal-to-noise, lower AGC the external attenuator affects only the signal, while the altimeter's AGC system is a measure of signal plus noise.

TABLE C-1. Analysis of the timed manual 1/2 dB AGC step changes, from GEOSAT Special Test data.

AGC Change Number	Meas. fr. edge in 1/60	Calc. AGC, in dB	New Change Number, n	Linear AGC, in dB	Calc. minus Linear
1	21.6	30.6	34	30.6	-0.05
2	22.2	31.2	35	31.1	0.05
3	22.7	31.7	36	31.6	0.05
4	23.1	32.1	37	32.1	-0.05
5	23.6	32.6	38	32.6	-0.05
6	24.0	33.0	39	33.1	-0.15
7	24.6	33.5	40	33.6	-0.05
8	25.1	34.0	41	34.1	-0.05
9	25.6	34.5	42	34.6	-0.05
10	26.1	35.0	43	35.1	-0.05
11	26.5	35.4	44	35.6	-0.16
12	27.0	35.9	45	36.1	-0.16
13	27.4	36.3	46	36.6	-0.26
14	28.0	36.9	47	37.1	-0.16
15	28.5	37.4	48	37.6	-0.16
16	28.9	37.8	49	38.1	-0.26
17	29.5	38.4	50	38.6	-0.16
18	30.1	39.0	51	39.1	-0.06
19	30.5	39.4	52	39.6	-0.16
20	31.0	39.9	53	40.1	-0.16
21	31.5	40.4	54	40.6	-0.17
22	32.0 *	40.9	55	41.1	-0.17
23	32.5	41.4	56	41.6	-0.17
24	33.0	41.9	57	42.1	-0.17
25	33.5	42.4	58	42.6	-0.17
26	34.2	43.1	59	43.1	0.03
27	34.7	43.6	60	43.6	0.03
28	35.2	44.1	61	44.1	0.03
29	35.6	44.5	62	44.6	-0.07
30	36.0	44.9	63	45.1	-0.18
31	36.6	45.5	64	45.6	-0.08
32	37.1	46.0	65	46.1	-0.08
33	37.6	46.5	66	46.6	-0.08
34	38.1	47.0	67	47.1	-0.08
35	38.7	47.6	68	47.6	0.02
36	39.2	48.1	69	48.1	0.02
37	39.6	48.5	70	48.6	-0.08
38	40.2	49.1	71	49.1	0.02
39	40.7	49.6	72	49.6	0.02
40	41.2	50.1	73	50.1	0.01
41	41.8	50.7	74	50.6	0.11
42	42.3	51.2	75	51.1	0.11
43	42.6	51.5	76	51.6	-0.09
44	43.1	52.0	77	52.1	-0.09
45	43.6	52.5	78	52.6	-0.09
46	44.1	53.0	79	53.1	-0.09

TABLE C-1 continued

AGC Change Number	Meas. fr. edge in 1/60	Calc. AGC in dB	New Change Number, n	Linear AGC, in dB	Calc. minus Linear
47	44.6	53.5	80	53.6	-0.09
48	45.0	53.9	81	54.1	-0.19
49	44.5	53.4	80	53.6	-0.19
50	44.1	53.0	79	53.1	-0.09
51	43.6	52.5	78	52.6	-0.09
52	43.1	52.0	77	52.1	-0.09
53	42.7	51.6	76	51.6	0.01
54	42.2	51.1	75	51.1	0.01
55	41.7	50.6	74	50.6	0.01
56	41.2	50.1	73	50.1	0.01
57	40.7	49.6	72	49.6	0.02
58	40.2	49.1	71	49.1	0.02
59	39.6	48.5	70	48.6	-0.08
60	39.2	48.1	69	48.1	0.02
61	38.6	47.5	68	47.6	-0.08
62	38.1	47.0	67	47.1	-0.08
63	37.6	46.5	66	46.6	-0.08
64	37.0	45.9	65	46.1	-0.18
65	36.5	45.4	64	45.6	-0.18
66	36.1	45.0	63	45.1	-0.08
67	35.6	44.5	62	44.6	-0.07
68	35.1	44.0	61	44.1	-0.07
69	34.5	43.4	60	43.6	-0.17
70	34.0	42.9	59	43.1	-0.17
71	33.5	42.4	58	42.6	-0.17
72	33.0	41.9	57	42.1	-0.17
73	32.4	41.3	56	41.6	-0.27
74	31.9	40.8	55	41.1	-0.27
75	31.4	40.3	54	40.6	-0.27
76	30.9	39.8	53	40.1	-0.26
77	30.5	39.4	52	39.6	-0.16
78	30.0	38.9	51	39.1	-0.16
79	29.4	38.3	50	38.6	-0.26
80	28.9	37.8	49	38.1	-0.26
81	28.4	37.3	48	37.6	-0.26
82	27.9	36.8	47	37.1	-0.26
83	27.5	36.4	46	36.6	-0.16
84	27.0	35.9	45	36.1	-0.16
85	26.5	35.4	44	35.6	-0.16
86	26.1	35.0	43	35.1	-0.05
87	25.5	34.4	42	34.6	-0.15
88	25.0	33.9	41	34.1	-0.15
89	24.5	33.4	40	33.6	-0.15
90	24.0	33.0	39	33.1	-0.15
91	23.5	32.5	38	32.6	-0.15
92	23.0	32.0	37	32.1	-0.15
93	22.7	31.7	36	31.6	0.05

TABLE C-1 continued

AGC Change Number	Meas. fr. edge in 1/60	Calc. AGC, in dB	New Change Number, n	Linear AGC, in dB	Calc. minus Linear
94	22.2	31.2	35	31.1	0.05
95	21.6	30.6	34	30.6	-0.05
96	21.1	30.1	33	30.1	-0.04
97	20.6	29.6	32	29.6	-0.04
98	20.0	29.0	31	29.1	-0.14
99	19.6	28.6	30	28.6	-0.04
100	19.1	28.1	29	28.1	-0.04
101	18.6	27.6	28	27.6	-0.04
102	18.1	27.1	27	27.1	-0.04
103	17.6	26.6	26	26.6	-0.04
104	17.0	26.0	25	26.1	-0.14
105	16.5	25.5	24	25.6	-0.13
106	16.1	25.1	23	25.1	-0.03
107	15.6	24.6	22	24.6	-0.03
108	15.1	24.1	21	24.1	-0.03
109	14.7	23.7	20	23.6	0.07
110	14.2	23.2	19	23.1	0.07
111	13.7	22.7	18	22.6	0.07
112	13.2	22.2	17	22.1	0.07
113	12.7	21.7	16	21.6	0.07
114	12.2	21.2	15	21.1	0.07
115	11.8	20.8	14	20.6	0.18
116	11.4	20.4	13	20.1	0.28
117	11.0	20.0	12	19.6	0.38
118	10.6	19.6	11	19.1	0.48
119	10.2	19.2	10	18.6	0.58
120	9.7	18.7	9	18.1	0.58
121	9.3	18.3	8	17.6	0.68
122	8.8	17.8	7	17.1	0.68
123	8.4	17.4	6	16.6	0.78
124	7.9	16.9	5	16.1	0.78
125	7.5	16.5	4	15.6	0.88
126	7.2	16.2	3	15.1	1.08
127	6.8	15.8	2	14.6	1.19
128	6.6	15.6	1	14.1	1.49
129	6.8	15.8	2	14.6	1.19
130	7.2	16.2	3	15.1	1.08
131	7.5	16.5	4	15.6	0.88
132	7.9	16.9	5	16.1	0.78
133	8.3	17.3	6	16.6	0.68
134	8.8	17.8	7	17.1	0.68
135	9.2	18.2	8	17.6	0.58
136	9.7	18.7	9	18.1	0.58
137	10.2	19.2	10	18.6	0.58
138	10.5	19.5	11	19.1	0.38
139	10.9	19.9	12	19.6	0.28

TABLE C-1 continued

AGC Change Number	Meas. fr. edge in 1/60	Calc. AGC in dB	New Change Number, n	Linear AGC, in dB	Calc. minus Linear
140	11.4	20.4	13	20.1	0.28
141	11.8	20.8	14	20.6	0.18
142	12.2	21.2	15	21.1	0.07
143	12.7	21.7	16	21.6	0.07
144	13.2	22.2	17	22.1	0.07
145	13.7	22.7	18	22.6	0.07
146	14.2	23.2	19	23.1	0.07
147	14.7	23.7	20	23.6	0.07
148	15.1	24.1	21	24.1	-0.03
149	15.6	24.6	22	24.6	-0.03
150	16.0	25.0	23	25.1	-0.13
151	16.5	25.5	24	25.6	-0.13
152	17.0	26.0	25	26.1	-0.14
153	17.5	26.5	26	26.6	-0.14
154	18.0	27.0	27	27.1	-0.14
155	18.6	27.6	28	27.6	-0.04
156	19.0	28.0	29	28.1	-0.14
157	19.5	28.5	30	28.6	-0.14
158	20.0	29.0	31	29.1	-0.14
159	20.5	29.5	32	29.6	-0.14
160	21.0	30.0	33	30.1	-0.14
161	21.5	30.5	34	30.6	-0.14
162	22.1	31.1	35	31.1	-0.05
163	22.5	31.5	36	31.6	-0.15
164	22.9	31.9	37	32.1	-0.25
165	23.3	32.3	38	32.6	-0.35

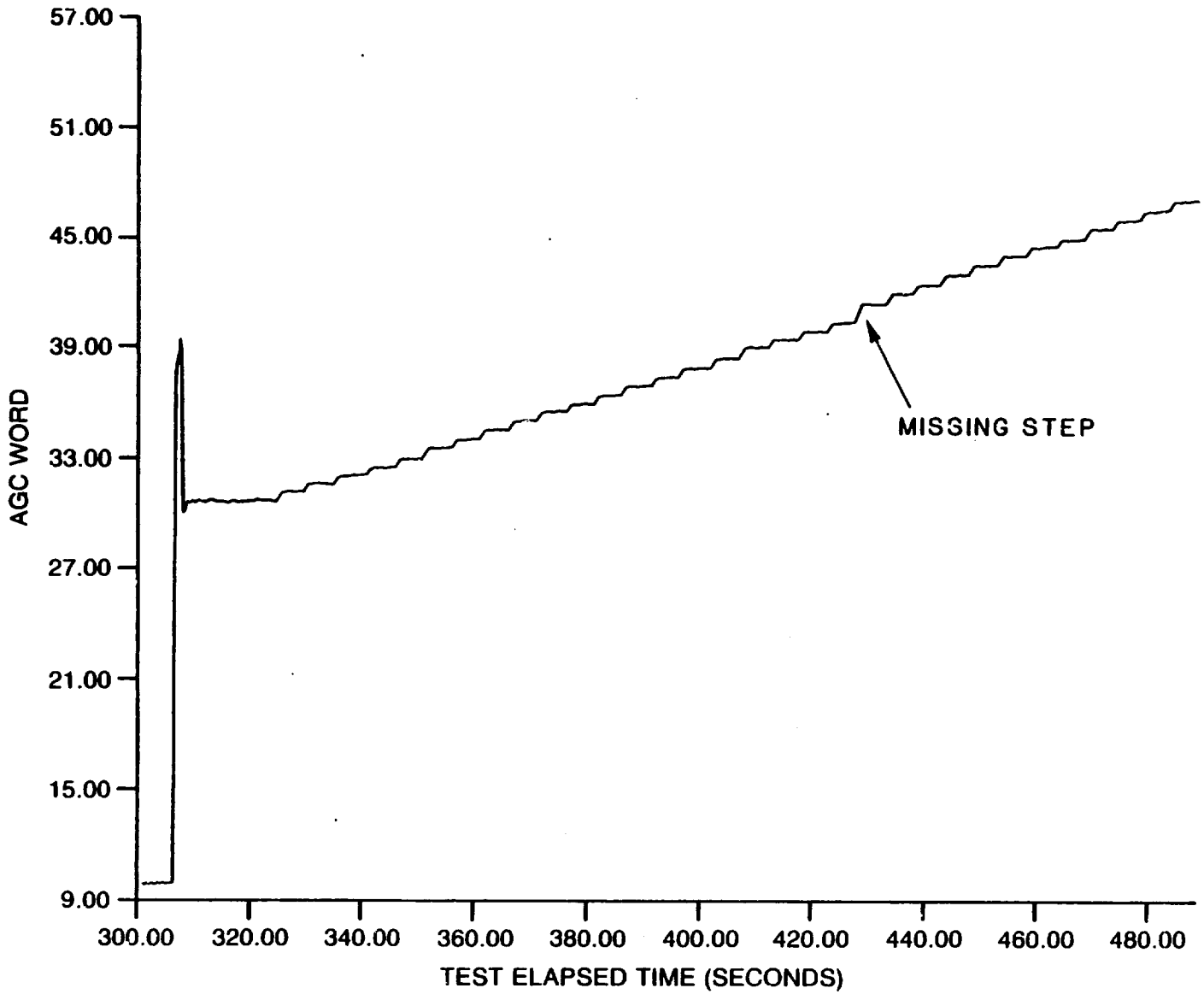

Fig. C1 — Part of the AGC data for GEOSAT special test 3C 09/01/83

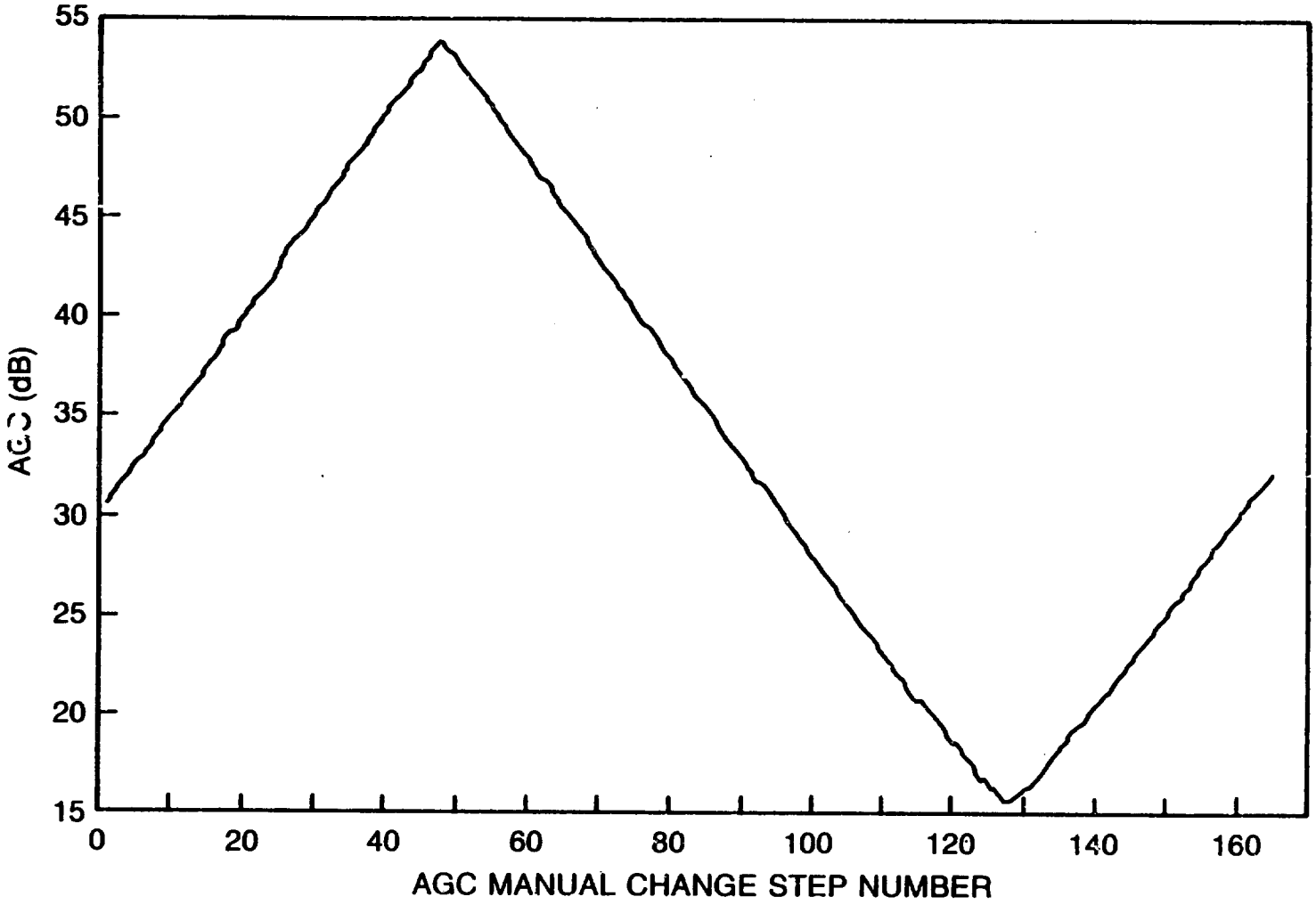

Fig. C2 — AGC vs. manual change step number

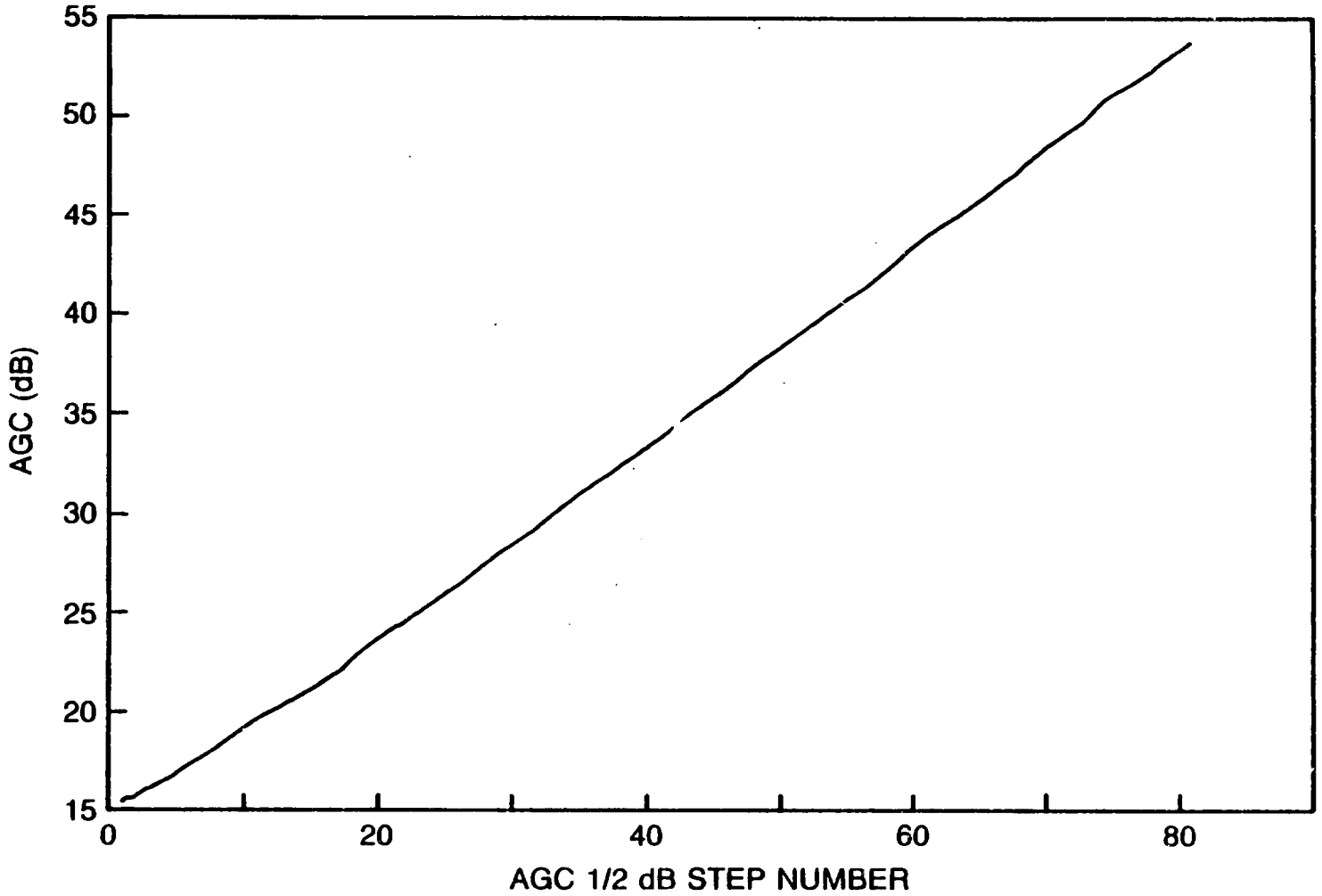

Fig. C3 — AGC vs. attenuation step number

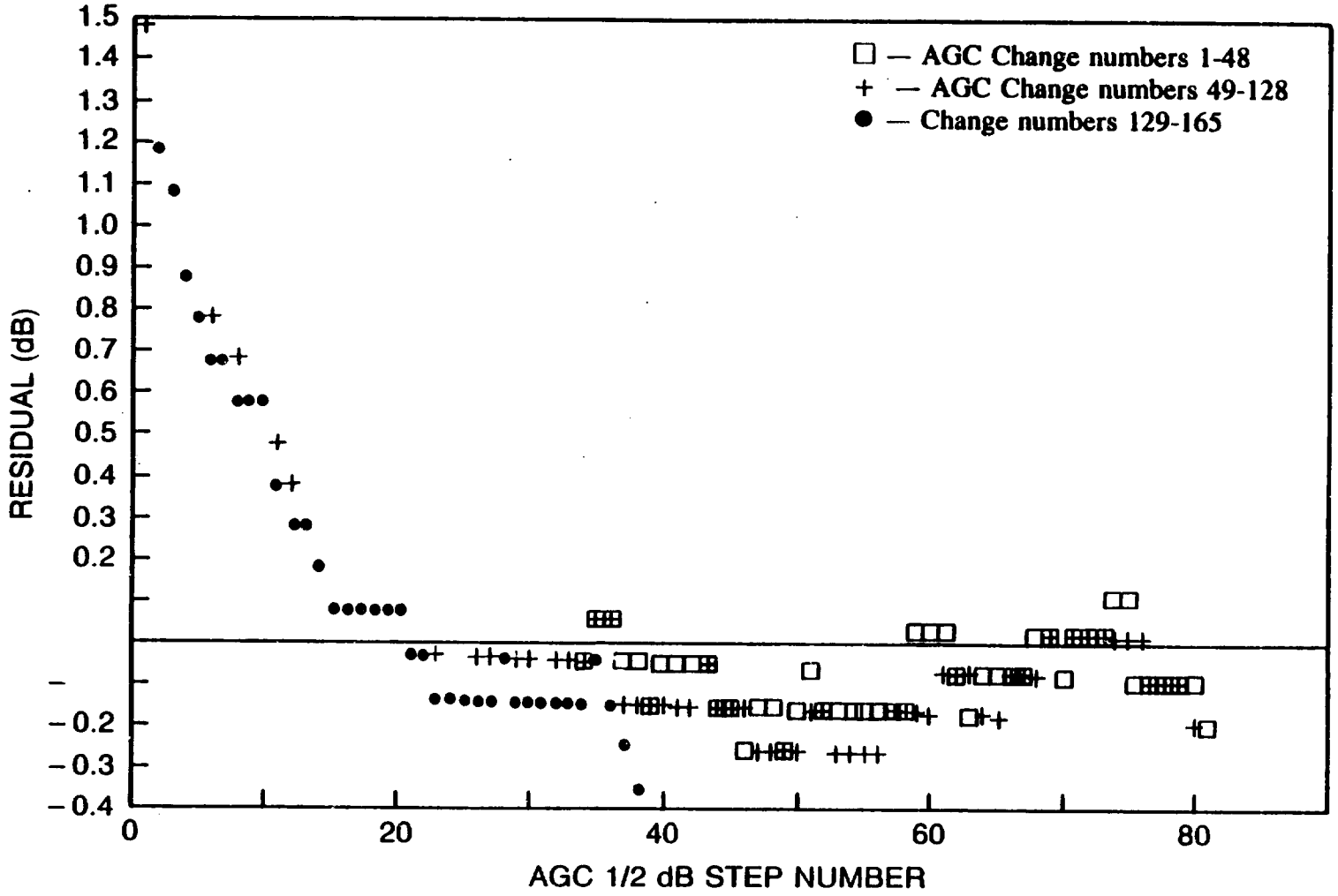

Fig. C4 — AGC residuals from straight line

Appendix D

Test Data I (9-1-83), segment 1A and 2B V_{att} values

5 sec. average	30 sec. average	210 sec. average
1.806	1.797	1.799
1.800	1.793	1.796
1.778	1.809	1.794
1.787	1.797	1.801
1.791	1.792	1.799
1.799	1.795	1.802
1.800	1.797	1.807
1.798	1.794	1.797
1.790	1.797	1.797
1.790	1.795	1.8
1.777	1.801	1.801
1.804	1.805	1.801
1.809	1.804	
1.822		
1.789		
1.817		
1.796		
1.806		
1.796		
1.806		
1.786		
1.804		
1.793		
1.800		
1.794		
1.788		
1.808		
1.773		
1.776		
1.788		
1.815		
1.799		
1.797		
1.803		
1.785		
1.776		
1.776		
1.802		
1.806		
1.792		
1.801		